The Plant Cell, Vol. 27: 86–103, January 2015, www.plantcell.org © NRC Canada 2015

LARGE-SCALE BIOLOGY ARTICLE

Understanding the Biochemical Basis of Temperature-Induced Lipid Pathway Adjustments in Plants

Qiang Li,[a,b] Qian Zheng,[a] Wenyun Shen,[a] Dustin Cram,[a] D. Brian Fowler,[c] Yangdou Wei,[b] and Jitao Zou[a,1]

[a] National Research Council Canada, Saskatoon, Saskatchewan S7N 0W9, Canada
[b] Department of Biology, University of Saskatchewan, Saskatoon, Saskatchewan S7N 5E2, Canada
[c] Department of Plant Sciences, University of Saskatchewan, Saskatoon, Saskatchewan S7N 5A8, Canada

Glycerolipid biosynthesis in plants proceeds through two major pathways compartmentalized in the chloroplast and the endoplasmic reticulum (ER). The involvement of glycerolipid pathway interactions in modulating membrane desaturation under temperature stress has been suggested but not fully explored. We profiled glycerolipid changes as well as transcript dynamics under suboptimal temperature conditions in three plant species that are distinctively different in the mode of lipid pathway interactions. In *Arabidopsis thaliana*, a 16:3 plant, the chloroplast pathway is upregulated in response to low temperature, whereas high temperature promotes the eukaryotic pathway. Operating under a similar mechanistic framework, *Atriplex lentiformis* at high temperature drastically increases the contribution of the eukaryotic pathway and correspondingly suppresses the prokaryotic pathway, resulting in the switch of lipid profile from 16:3 to 18:3. In wheat (*Triticum aestivum*), an 18:3 plant, low temperature also influences the channeling of glycerolipids from the ER to chloroplast. Evidence of differential trafficking of diacylglycerol moieties from the ER to chloroplast was uncovered in three plant species as another layer of metabolic adaptation under temperature stress. We propose a model that highlights the predominance and prevalence of lipid pathway interactions in temperature-induced lipid compositional changes.

INTRODUCTION

Glycerolipid, as the principle constituent of cellular membranes, has been a focus of attention since the 1960s in the context of temperature adaptation in plants (Wolfe, 1978; Harwood, 1991). A considerable body of work was centered on the metabolic step of fatty acid desaturation in response to temperature fluctuations, namely, the activities of various fatty acid desaturases (Murata et al., 1992; Murata and Los, 1997; Murakami et al., 2000; Iba, 2002; Wallis and Browse, 2002). However, the link between fatty acid desaturases and modulation of desaturation under temperature stress remains a weak one. A straightforward correlation between lipid unsaturation and expression could not be found for most desaturase genes, except *FATTY ACID DESATURASE8* (*FAD8*) (Matsuda et al., 2005).

In plant cells, fatty acid biosynthesis takes place exclusively in chloroplasts. However, two discrete glycerolipid assembly pathways exist separately in the chloroplast and the cytoplasmic compartment, generally known as the prokaryotic and the eukaryotic pathway, respectively (Browse et al., 1986; Ohlrogge and Browse, 1995). Owing to the substrate specificity of the chloroplast lysophosphatidic acyltransferase, the prokaryotic pathway in the chloroplast generates glycerolipids with a C16 fatty acyl moiety at the *sn-2* position. The eukaryotic pathway, by contrast, produces glycerolipid molecules that have only C18 fatty acid at *sn-2*. The two pathways are compartmentalized by membrane barriers, but coordinate closely to meet the overall demand of cellular membrane biogenesis and maintenance (Kunst et al., 1988; Ohlrogge and Browse, 1995). However, there is considerable flexibility in the relative contributions of the two pathways to overall glycerolipid production. In species such as *Arabidopsis thaliana* and spinach (*Spinacia oleracea*), biosynthesis of major chloroplast lipids, particularly monogalactosyldiacylglycerol (MGDG) and digalactosyldiacylglycerol (DGDG), draws nearly equal contribution from the two pathways (Ohlrogge and Browse, 1995). The *sn-2* C16 fatty acyl moiety in MGDG and DGDG produced through the prokaryotic pathway undergoes a series of desaturations, leading to the formation of 16:3 fatty acid. Plant species that rely on a significant contribution from the prokaryotic pathway for chloroplast lipid biosynthesis are therefore called 16:3 plants. By contrast, plants such as pea (*Pisum sativum*) and wheat (*Triticum aestivum*), wherein, besides phosphatidylglycerol (PG), the biosynthesis of chloroplast glycerolipids are almost entirely dependent on the eukaryotic pathway, are classified as 18:3 plants (Heinz and Roughan, 1983; Browse et al., 1986; Ohlrogge and Browse, 1995).

Studies show that membrane lipid biosynthesis is robust and well maintained even in the face of genetic lesions of major metabolic steps (Browse et al., 1986; Johnson and Williams, 1989; Brockman et al., 1990; Somerville and Browse, 1991; Härtel et al., 2000). For example, the *Arabidopsis act1* mutant, deficient in the activity of the chloroplast glycerol-3-phosphate acyltransferase, is

[1] Address correspondence to jitao.zou@nrc-cnrc.gc.ca.
The author responsible for distribution of materials integral to the findings presented in this article in accordance with the policy described in the Instructions for Authors (www.plantcell.org) is: Jitao Zou (jitao.zou@nrc-cnrc.gc.ca).
www.plantcell.org/cgi/doi/10.1105/tpc.114.134338

essentially devoid of 16:3-containing MGDG from the prokaryotic pathway. However, the proportions of various classes of glycerolipids in *act1* were similar to those of the wild type due to an apparent increase in the trafficking of endoplasmic reticulum (ER) lipids to chloroplasts (Kunst et al., 1988). A notable case illustrating the biological significance of a highly coordinated and flexible pathway adjustment is that of metabolic response to phosphate deprivation in *Arabidopsis* (Benning et al., 2006; Benning, 2009). Under phosphate starvation, phospholipids are replaced by galactolipids in not only the thylakoid membrane, but also the extraplastidic membranes (Härtel et al., 2000), thereby reducing the need for phosphorus consumption for membrane lipid biosynthesis. Proportional changes of glycerolipid species have also been documented in plants subjected to temperature fluctuations (Pearcy, 1978; Johnson and Williams, 1989; Harwood, 1991, 1994; Chen et al., 2006). An increased proportion of DGDG was observed at high temperature in *Arabidopsis* (Chen et al., 2006), whereas biosynthesis of MGDG in canola (*Brassica napus*) was induced by low temperature (Johnson and Williams, 1989).

Modular regulations of the two glycerolipid pathways in response to metabolic perturbations are evident not only in glycerolipid profiles but also at the transcript level of many enzymatic components associated with the two pathways (Shen et al., 2010). Most recently, strictly coordinated gene expression at the biochemical pathway level in parallel with changes of specific glycerolipid pools was reported in *Arabidopsis* in response to light and temperature stimuli (Szymanski et al., 2014). Nonetheless, how glycerolipid composition is mechanistically modulated between the two glycerolipid pathways and precisely what factors are involved in this process remain largely unknown. In this study, we explored the significance of glycerolipid pathway balance in temperature-induced lipid compositional changes in three plant species that have distinctive modes of lipid pathway interactions. In *Arabidopsis*, a typical 16:3 plant, low temperature induces an augmented prokaryotic pathway, whereas high temperature enhances the eukaryotic pathway. *Atriplex lentiformis* switches lipid profile from 16:3 to 18:3 when it encounters heat and reduces its overall lipid desaturation through drastically increasing the contribution of the eukaryotic pathway. In wheat, which is an 18:3 plant, low temperature causes a reduced contribution from the ER pathway to chloroplast lipid biosynthesis. In sync with the metabolic changes is coordinated expression of glycerolipid pathway genes at the transcript level. Our study demonstrates that metabolic adjustments from different intracellular glycerolipid pathways represent a major regulatory mechanism through which the provision of lipid substrates for membrane desaturation is regulated under temperature stress.

RESULTS

Experimental Setup and Metabolite and Transcriptome Data Acquisition

Three plant species were used in this study. *Arabidopsis*, a model 16:3 plant, was raised at low (10°C), high (30°C), or standard (22°C) growth temperature, under similar light intensity and with an identical light cycle (16 h/8 h). Wheat, a 18:3 plant and a valuable system in which to assess metabolic response to low temperature in cold adaptation and cold acclimation for freezing tolerance (Limin and Fowler, 2006; Fowler, 2008), was grown at 23°C for 2 weeks (control) and then shifted to 4°C for another 2 weeks. *A. lentiformis* of the *Chenopodiaceae* family is a unique species in regard to fatty acid phenotype: It switches from that of a 16:3 plant to 18:3 under extreme heat. To assess the effect of high temperature, *A. lentiformis* plants were grown at 23°C or 43°C for 8 weeks (Pearcy, 1978).

Lipid compositions of *Arabidopsis*, *A. lentiformis*, and wheat grown at various temperatures were quantitatively assessed by thin layer chromatography (TLC)-based lipid analysis. Glycerolipids were first separated by two-dimensional TLC (2D-TLC), followed by gas chromatography quantification of fatty acid methyl esters (Shen et al., 2010). Relative contributions of the prokaryotic and eukaryotic pathways were then delineated through stereo-specific analysis of fatty acid distribution in various lipid classes (Shen et al., 2010). Metabolite profiles for *A. lentiformis* and wheat were further interrogated at the level of head group, carbon chain length, and double bonds of the acyl groups through electrospray ionization tandem mass spectrometry (ESI-MS/MS) (Welti et al., 2002). Transcript analysis in *Arabidopsis* was performed with quantitative RT-PCR (qRT-PCR) on selected genes (Shen et al., 2010). High-throughput RNA sequencing (RNA-seq) was employed to explore pathway adjustments in *A. lentiformis* and wheat.

Effect of Suboptimal Temperature on Glycerolipid Profile and Fatty Acid Composition in *Arabidopsis*

Mol % of major fatty acid in *Arabidopsis* under different temperature treatments is shown in Supplemental Figure 1. Both 16:3 and 18:3 polyunsaturated fatty acids decreased at 30°C, while at 10°C, the polyunsaturated 18:3 fatty acid increased. The proportion of 18:2 fatty acids increased at 30°C and decreased at 10°C. The monounsaturated 18:1 fatty acid was detected at an elevated level under either 10°C or 30°C when compared with standard growth temperature of 22°C.

Analysis of individual lipid classes revealed distinctive effects of high and low temperature on the relative proportion of glycerolipid classes. MGDG displayed an increase at 10°C, while increased DGDG was observed at high temperature (30°C) (Supplemental Table 1). Major phospholipids, phosphatidylcholine (PC) and phosphatidylethanolamine (PE), showed decreases at either high or low temperature. In reference to standard growth temperature, the proportion of galactolipids was increased, while the content of phospholipid species was decreased, irrespective of high or low growth temperature.

We next analyzed the fatty acyl compositions of individual lipid classes (Supplemental Table 1). The most notable change was an increase in the ratio of 18:3/18:2 at 10°C in all glycerolipid classes. A decreased 18:3/18:2 ratio, on the other hand, was observed at 30°C. Double bond index (DBI) calculations illustrated a trend of increase at 10°C and a decrease at 30°C in each lipid class (Supplemental Figure 2). DGDG, PE, and sulfoquinovosyl diacylglycerol (SQDG) had a lower C16/C18 ratio at 10°C and a higher ratio at 30°C when compared with 22°C. MGDG showed an opposite response, with increased

C16/C18 ratio at 10°C and decreased ratio at 30°C (Supplemental Table 1).

Contrasting Glycerolipid Pathway Partitioning Patterns in *Arabidopsis* Grown at 10°C and 30°C

To quantify the relative contributions of the two glycerolipid pathways under suboptimal temperature conditions, purified lipids were digested with *Rhizopus* sp lipase to *lyso*-derivatives from which stereo-specific fatty acid distribution was then determined (Figure 1). A previously detailed analysis of *Arabidopsis* showed that for every 1000 fatty acid molecules produced in the chloroplast, 615 enter the eukaryotic pathway (Browse et al., 1986; Miquel et al., 1998). We performed similar analysis with plants grown at each growth temperature. This revealed (Table 1) an enhanced contribution from the prokaryotic pathway for MGDG biosynthesis at 10°C and a reduced input from the eukaryotic pathway when compared with plants at 22°C. At 30°C, the contribution from the ER pathway for both MGDG and DGDG biosynthesis was increased. Hence, high temperature enhanced the eukaryotic pathway contribution of diacylglycerol (DAG) moieties to galactolipid biosynthesis, while low temperature enhanced the prokaryotic pathway contribution, primarily to MGDG.

Modular Regulation of the Two Glycerolipid Pathways at the Transcript Level under High and Low Temperature

We selected 24 *Arabidopsis* genes (Shen et al., 2010) for real-time qRT-PCR to gain insight into metabolic readjustments at the transcript level (Figure 2). Consistent with metabolite analysis, transcript for the plastidic glycerol-3-phosphate acyltransferase (*ACT1*) was detected at an elevated level (1.6-fold) at 10°C. Several genes involved in MGDG biosynthesis were also induced, including *MONOGALACTOSYL DIACYLGLYCEROL SYNTHASE1* (*MGD1*; 1.6-fold), *FAD5* (4.6-fold), and *FAD8* (1.8-fold). Transcript for the main DGDG synthase, *DGD1*, showed a 1.9-fold increase at 10°C when compared with 22°C. Evidence consistent with a reduced eukaryotic pathway contribution at low temperature was seen with *FAD2*, which exhibited a decrease of 2.3-fold.

A reverse trend of transcript level changes was observed at high temperature. Several genes of the eukaryotic pathway were induced. For example, *FAD2* was upregulated 1.8-fold. *PHOSPHATIDYLINOSITOL SYNTHASE1* (*ATPIS1*), which encodes an enzyme that uses DAG originating from the eukaryotic pathway to produce phosphatidylinositol (PI), was also increased (1.6-fold). Consistent with increased DGDG from the eukaryotic pathway, the level of *DGD2* was increased (2.3-fold). There were no significant changes in SQDG content under the temperature conditions we tested

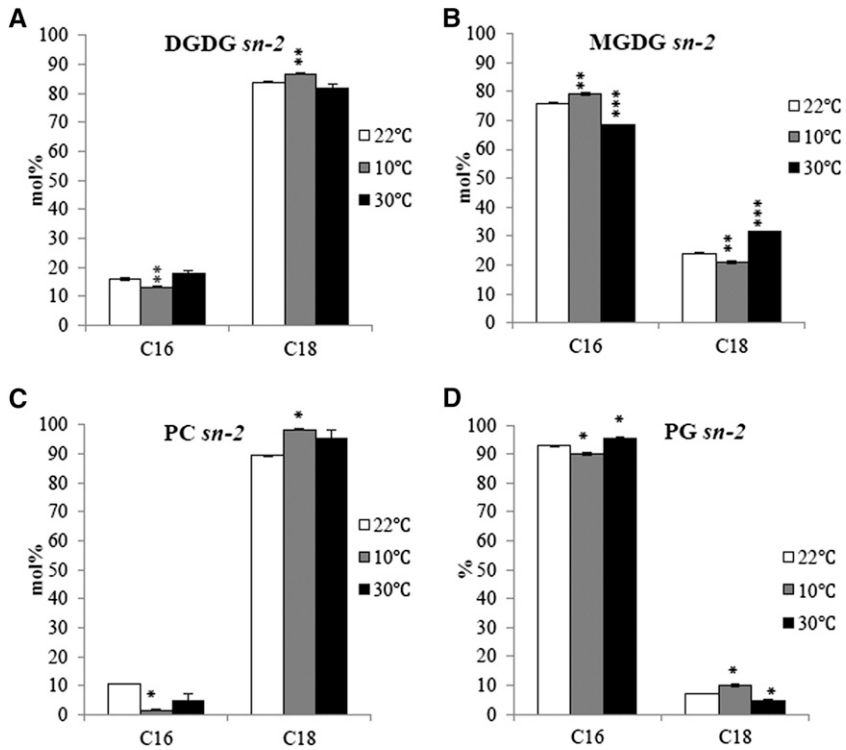

Figure 1. Stereo-Specific Analyses of Glycerolipid Molecules Originating from the Eukaryotic and Prokaryotic Pathways.

The *lyso*-lipids (representing the *sn-2* position of the parent lipid) were purified by TLC and derivatized using 3 N methanolic HCl and analyzed by gas chromatography. DGDG **(A)**; MGDG **(B)**; PC **(C)**; PG **(D)**. C16 represents the sum of 16: l, 16:2, and 16:3; C18 represents the sum of 18:0, 18:1, 18:2, and 18:3. Values are means ± SD (n = 3). Statistically significant differences were calculated in comparison to the standard growth condition (22°C). Two-tailed Student's t test; *P < 0.05; **P < 0.01; ***P < 0.001.

Table 1. Mass Composition and Fatty Acid Flux Sharing between the Two Glycerolipid Pathways in *Arabidopsis* Grown at 10, 22, and 30°C

	Mass of Fatty Acid (mol/1000 mol)[a]	*sn*-2 Position (%)[b]		Fatty Acid Entering Prokaryotic Pathway (mol/1000 mol Fatty Acid)	Fatty Acid Entering Eukaryotic Pathway (mol/1000 mol Fatty Acid)
		C16	C18		
MGDG					
10°C	411	79	21	325	86
22°C	380	76	24	289	91
30°C	387	68	32	263	124
DGDG					
10°C	159	13	87	21	138
22°C	160	16	84	26	134
30°C	179	18	82	32	147
PC					
10°C	166	2	98	3	163
22°C	176	8	92	14	162
30°C	161	4	96	6	155
PG					
10°C	101	90	10	91	10
22°C	101	93	7	94	7
30°C	103	95	5	98	5
PE					
10°C	114	0	100	0	114
22°C	124	0	100	0	124
30°C	106	0	100	0	106
PI					
10°C	30	0	100	0	30
22°C	35	0	100	0	35
30°C	35	0	100	0	35
SQDG					
10°C	20	100	0	20	0
22°C	23	100	0	23	0
30°C	28	100	0	28	0
Total					
10°C	1000			460	540
22°C	1000			445	555
30°C	1000			428	572

Data were calculated based on results of Supplemental Table 1 and Figure 1 according to methods of Browse et al. (1986) and Shen et al. (2010). C16 represents the sum of 16:0, 16:l, 16:2, and 16:3; C18 represents the sum of 18:0, 18:1, 18:2, and 18:3.

[a]An original input of 1000 mole of fatty acids biosynthesized in the chloroplast as acyl-ACP species.

[b]Each lipid species was divided between the prokaryotic and eukaryotic pathways on the basis of content of C16 at the *sn*-2 position.

(Supplemental Table 1). However, the expression of the two SQDG synthases, *SQD1* and *SQD2*, appeared to be both induced at 30°C.

Consistent with previous findings (Matsuda et al., 2005), *FAD8*, encoding the only fatty acid desaturase among the eight with confirmed regulation by temperature, was induced at low temperature and repressed at high temperature. The expression of *FAD2*, which encodes the ER-based ω-6 desaturase responsible for the conversion of 18:1 to 18:2 in PC, was upregulated at 30°C and downregulated at 10°C. Underscoring the significance of *FAD2* transcript changes was the level of 18:2 in PC, which clearly decreased at 10°C while increased at 30°C (Supplemental Table 1).

Conversion from 16:3 to 18:3 Lipid Profile in *A. lentiformis* Operates through Pathway Adjustment

Despite the unequivocal definition of 16:3 and 18:3 plants, clear classification of the two categories required an arbitrary threshold for 16:3 (Mongrand et al., 1998). 16:3 plants are classified as those with more than 2 mol % of 16:3 in total fatty acids or 3 mol % and 1.2 mol % in MGDG and DGDG, respectively (Mongrand et al., 1998). *A. lentiformis* represents a notable exception. It is a typical 16:3 plant in coastal regions of California but switches to 18:3 when grown in desert and high temperature habitat (Pearcy, 1978). That its prokaryotic pathway was repressed at high temperature was previously suggested (Kunst et al., 1989) but not verified. We raised *A. lentiformis* at 23°C or 43°C in two growth chambers with similar light conditions. Analyses of leaf tissues of 8-week-old plants confirmed a decrease of 16:3 from 5.5 mol % at 23°C to 0.9 mol % at 43°C (Supplemental Figure 3). We then examined changes in the proportions of each glycerolipid species (Supplemental Table 2). DGDG was increased at 43°C and almost entirely devoid of 16:3 (0.2 mol %). MGDG was decreased, and the level of 16:3 was reduced from 14.6 mol % at 23°C to 2.7 mol % at 43°C. The proportions of PC and PI were increased, whereas

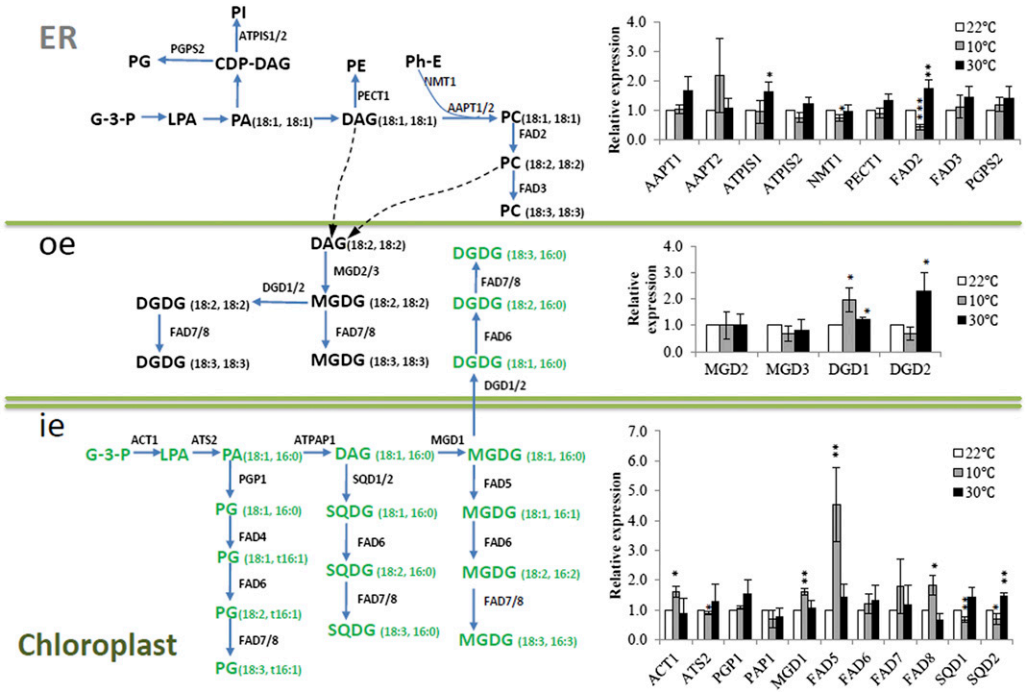

Figure 2. Glycerolipid Pathway Coordination at the Transcript Level.

Lipid species are generated through either the eukaryotic (*sn-1/sn-2*, C18/C18 or C16/C18) or the prokaryotic pathway (*sn-1/sn-2*, C18/C16). Dashed lines represent possible channeling between the ER and chloroplast (Benning, 2009). Relative expression levels of selected genes were analyzed by real-time qRT-PCR using cDNA from *Arabidopsis* grown at 22°C (white bar), 10°C (gray bar), and 30°C (black bar) as templates. For comparison, expression values from plants grown at 22°C were normalized to 1 using StepOne software 2.0 (Applied Biosystems). Relative expression values (means ± SD, $n = 3$) from low- and high-temperature-treated plants were presented as fold change against plants grown at 22°C. *P value < 0.05; **P value < 0.01 (two-tailed Student's *t* test) compared with values for control (plants grown at 22°C). ie, inner envelope; oe, outer envelope.

the content of PG was reduced. At 43°C, concurrent with decreased proportion of 18:3 (Supplemental Table 2), 16:0 in all lipid classes was increased. A simultaneous increase of 18:1 and 18:2 fatty acids was observed in DGDG, MGDG, and SQDG. Eukaryotic lipids PC, PE, and PI showed notable increase of 18:1, while 18:2 and 18:3 were decreased (Supplemental Table 2). The level of 18:1 in PG also increased at 43°C but 18:2 was unchanged (Supplemental Table 2).

Stereo-specific fatty acid distribution was examined to determine the origin of MGDG, DGDG, PC, and PG. There was a decrease in the proportion of *sn-2* C16 in DGDG (Figure 3A) and MGDG (Figure 3B) at 43°C, confirming a decreased contribution from the prokaryotic pathway. As expected, the majority (more than 96%) of fatty acyl moieties at the *sn-2* position of PC were C18 (Figure 3C). Despite a decrease in the proportion of total PG at 43°C, no difference in the ratio of C16 to C18 at the *sn-2* position of PG was detected (Figure 3D). Relative to plants grown at 23°C, the proportion of 18:1 at the *sn-2* of PC at 43°C was increased, while 18:2 and 18:3 were decreased.

Relative contributions of the two glycerolipid pathways in *A. lentiformis* grown at 23°C and 43°C are presented in Table 2. Fatty acid channeling through the prokaryotic pathway was clearly reduced, while the eukaryotic pathway was enhanced at 43°C. Reduction in prokaryotic contribution affected the total level of MGDG. The biosynthesis of DGDG, while increased in level, relied heavily on the eukaryotic pathway. Because PG was primarily (~94%) produced by the prokaryotic pathway, that the total amount of PG was reduced also suggested reduced activity of the prokaryotic pathway at 43°C. Overall, glycerolipid pathway adjustment in *A. lentiformis* when grown at 43°C operated in a similar framework as that observed in *Arabidopsis* under high temperature, albeit to a much greater extent. These experiments thus confirmed that the conversion of lipid profile from 16:3 to 18:3 in *A. lentiformis* under high temperature was a consequence of rebalancing of the two major glycerolipid pathways.

Evidence of Differential Channeling of DAG Moieties in *A. lentiformis* and *Arabidopsis*

We then took a metabolomics approach to further probe individual lipid molecule species within each subset of glycerolipids through ESI-MS/MS (Welti et al., 2002). Compositions of each lipid species in *A. lentiformis* at 43°C were similar in trend to 2D-TLC data where an increase in DGDG was accompanied by a decrease of MGDG (Figure 4A). The proportions of PC and PI were also increased. Analysis of fatty acid compositions of individual lipids revealed that DGDG and MGDG containing DAG moieties of 34:6 were reduced (Figures 4B and 4C). These DAG (34:6) moieties should only have a fatty acid composition of the 18:3(*sn-1*)/16:3(*sn-2*) from the prokaryotic pathway, thus agreeing

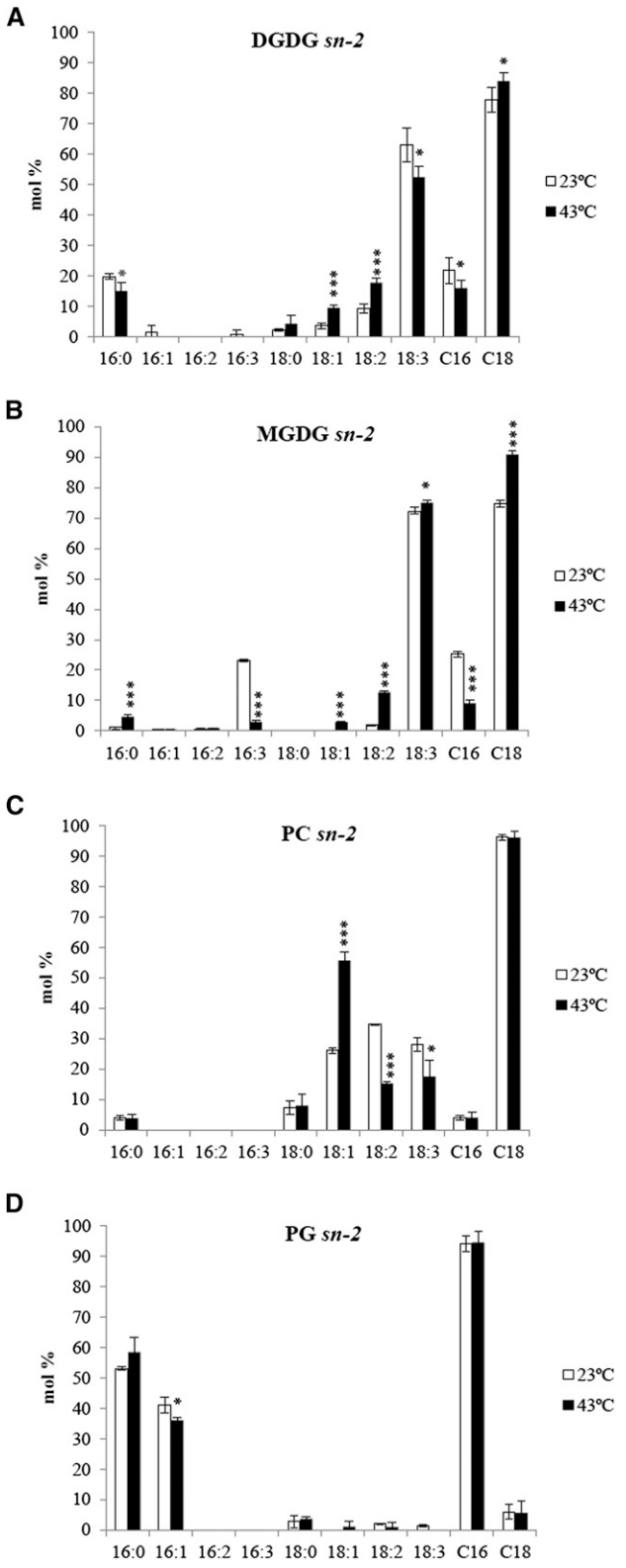

Figure 3. Stereo-Specific Analyses of Glycerolipids in *A. lentiformis* Grown at 23°C and 43°C.

with results of lipid class analysis that the prokaryotic pathway was repressed at 43°C.

We also noted that C34:1 (*sn-1* 16:0/ *sn-2* 18:1) phospholipid species, while barely detectable in *Arabidopsis* (Shen et al., 2010), were present in *A. lentiformis* at substantial levels (12 mol % in PC, 5 mol % in PE, and 10 mol % in PI at 23°C) (Supplemental Data Set 1). Moreover, C34:1 lipid species displayed drastic increases at 43°C, reaching 33 mol % in PC (Figure 4D), 19 mol % in PE, and 20 mol % in PI (Supplemental Data Set 1). Percentage of C34:1 lipid molecules in phosphatidic acid (PA) also increased from 8 to 23 mol % (Supplemental Data Set 1).

Along with the accumulation of C34:1 lipid molecules in phospholipids, there were corresponding increases of C34:3 lipid molecule species in both MGDG and DGDG, with its rise in DGDG being particularly pronounced (Figures 4B and 4C). An increased C34 and decreased C36 in PA were observed in *A. lentiformis* at 43°C (Supplemental Figure 4). This was significant in light of the potential precursor-product relationship between PA and DGDG and MGDG. Given that the prokaryotic pathway was largely repressed in *A. lentiformis* at 43°C (Table 2), the increased C34 lipid species should be produced through the eukaryotic pathway and have a molecular composition of 16:0/ 18:3 (*sn-1*/ *sn-2*). To verify this, we calculated *sn-1* fatty acyl composition based on results of *sn-2* stereo-specific analysis and the composition of total fatty acid. This confirmed that, at 43°C, there was consistently an increased 16:0 at the *sn-1* position of DGDG and MGDG (Figure 5A).

The above results prompted us to examine the *sn-1* distribution of 16:0 in DGDG and MGDG in *Arabidopsis*. As shown in Figure 5B, there was an increase of 16:0 at the *sn-1* of DGDG and MGDG at 30°C and a decrease of 16:0 at 10°C. An increase of DGDG (16:0/C18, *sn-1*/*sn-2*) in *Arabidopsis dgd1* mutants under phosphate-limiting condition has been observed, suggesting a selective channeling of C34 DAG for DGDG synthesis (Härtel et al., 2000). Given the molecular profile changes detected in PC and PA, we concluded that the increased DGDG (Supplemental Table 2) were derived, in large proportion, from eukaryotic lipids with 16:0 moieties at the *sn-1* position. It is noteworthy that C16/ C18 ratio was increased in DGDG (Supplemental Table 2), providing further evidence that there was proportionally a reduction of C18-containing DAG moieties in DGDG biosynthesis. Taken together, our results provide evidence for a differential channeling of C34 (C16/C18) and C36 (C18/C18) DAG moieties from the ER to the chloroplast during temperature adaptation in plants.

Pathway Coordination at the Transcriptome Level in *A. lentiformis*

To seek insight into factors regulating the shift from a 16:3 to an 18:3 lipid profile in *A. lentiformis*, we conducted RNA-seq analysis

C16 represents the sum of 16:l, 16:2, and 16:3; C18 represents the sum of 18:0, 18:1, 18:2, and 18:3. DGDG **(A)**; MGDG **(B)**; PC **(C)**; PG **(D)**. Values are means ± SD (n = 3). *P < 0.05; **P < 0.01; ***P < 0.001 (two-tailed Student's t test).

Table 2. Mass Composition and Fatty Acid Flux Sharing between the Two Glycerolipid Pathways in *A. lentiformis* Plants Grown at 23°C and 43°C

	Mass of Fatty Acid (mol/1000 mol)[a]	*sn*-2 Position (%)[b]		Fatty Acid Entering Prokaryotic Pathway (mol/1000 mol Fatty Acid)	Fatty Acid Entering Eukaryotic Pathway (mol/1000 mol Fatty Acid)
		C16	C18		
MGDG					
23°C	419	25	75	107	313
43°C	359	9	91	33	326
DGDG					
23°C	217	22	78	47	169
43°C	260	16	84	42	218
PC					
23°C	148	4	96	6	142
43°C	164	4	96	6	158
PG					
23°C	89	94	6	84	5
43°C	70	94	6	66	4
PE					
23°C	68	0	100	0	68
43°C	68	0	100	0	68
PI					
23°C	24	0	100	0	24
43°C	41	0	100	0	41
SQDG					
23°C	36	100	0	36	0
43°C	37	100	0	37	0
Total					
23°C	1000			279	721
43°C	1000			185	815

Data were calculated based on results of Supplemental Table 2 and Figure 3 according to Browse et al. (1986) and Shen et al. (2010). C16 represents the sum of 16:0, 16:l, 16:2, and 16:3; C18 represents the sum of 18:0, 18:1, 18:2, and 18:3.

[a]An original input of 1000 mole of fatty acids synthesized in the chloroplast as acyl-ACP species.

[b]Each lipid species was divided between the prokaryotic and eukaryotic pathway on the basis of C16 content at the *sn*-2 position.

to assess gene expression at 23°C and 43°C. Total RNA was extracted from 8-week-old leaf tissues with four biological replicates for each growth condition. After quality filtering, all reads were de novo assembled using Trinity (Grabherr et al., 2011; Haas et al., 2013) to construct the first *A. lentiformis* transcriptome. A total of 144,456 transcripts with an average length of 1109 bp were constructed and submitted to the Gene Expression Omnibus (http://www.ncbi.nlm.nih.gov/geo/). Of the 144,456 transcripts, 46,492 transcripts with at least 50 reads across eight samples were defined as expressed and were used for differential expression analysis (Supplemental Data Set 2). Putative functions of transcripts were assigned using BLASTx searches against the TAIR10 protein database and a cutoff E-value of 10^{-6}. Expression levels of lipid metabolism genes were compiled according to the Arabidopsis Acyl-Lipid Metabolism database (http://aralip.plantbiology.msu.edu) (Supplemental Data Set 3) (Beisson et al., 2003; Li-Beisson et al., 2013). In cases where more than one transcript hit the same AGI protein in *Arabidopsis*, transcript with the highest fragments per kilobase of exon per million fragments value (and presumably highest expression level) was assigned as a representative of the AGI group (Supplemental Data Set 4).

Consistent with lipid compositional analysis, *ACT1* transcript was reduced by 3.4-fold at 43°C. The level of *FAD5* was downregulated by 1.9-fold. Expression of *FAD7* was also reduced (1.5-fold). In line with a reduction of PG content, the chloroplast *CYTIDINEDIPHOSPHATE DIACYLGLYCEROL SYNTHASE4* involved in PG biosynthesis was suppressed (2.3-fold). Demonstrating once again a positive correlation with the contribution of the eukaryotic pathway, the transcript of *FAD2* was upregulated (2.2-fold) at 43°C. Expression of *PHOSPHATIDYLINOSITOL SYNTHASE1* was upregulated 2.4-fold, which was consistent with an increased amount of PI at high temperature. Hence, transcript levels of glycerolipid pathway enzymes in the ER and chloroplast were regulated *en bloc* to achieve the conversion of lipid profile from 16:3 to 18:3. Importantly, *FAD2*, *FAD5*, and *ACT1*, identified previously as key genes influencing glycerolipid pathway balance in *Arabidopsis*, were recaptured in *A. lentiformis*.

Changes in fatty acid synthesis and lipid trafficking related genes were also detected. *STEAROYL-ACYL-CARRIER-PROTEIN DESATURASE5* (*DES5*), which mediates the desaturation of 18:0-ACP to 18:1-ACP in chloroplasts, was upregulated 5.2-fold at high temperature. *FATTY ACYL-ACP THIOESTERASES B* (*FaTB*) was downregulated 2.4-fold. Increased rates of fatty acid synthesis and increased exports of 18:1 from chloroplast to the ER have been observed in *Arabidopsis fatb* mutants (Bonaventure

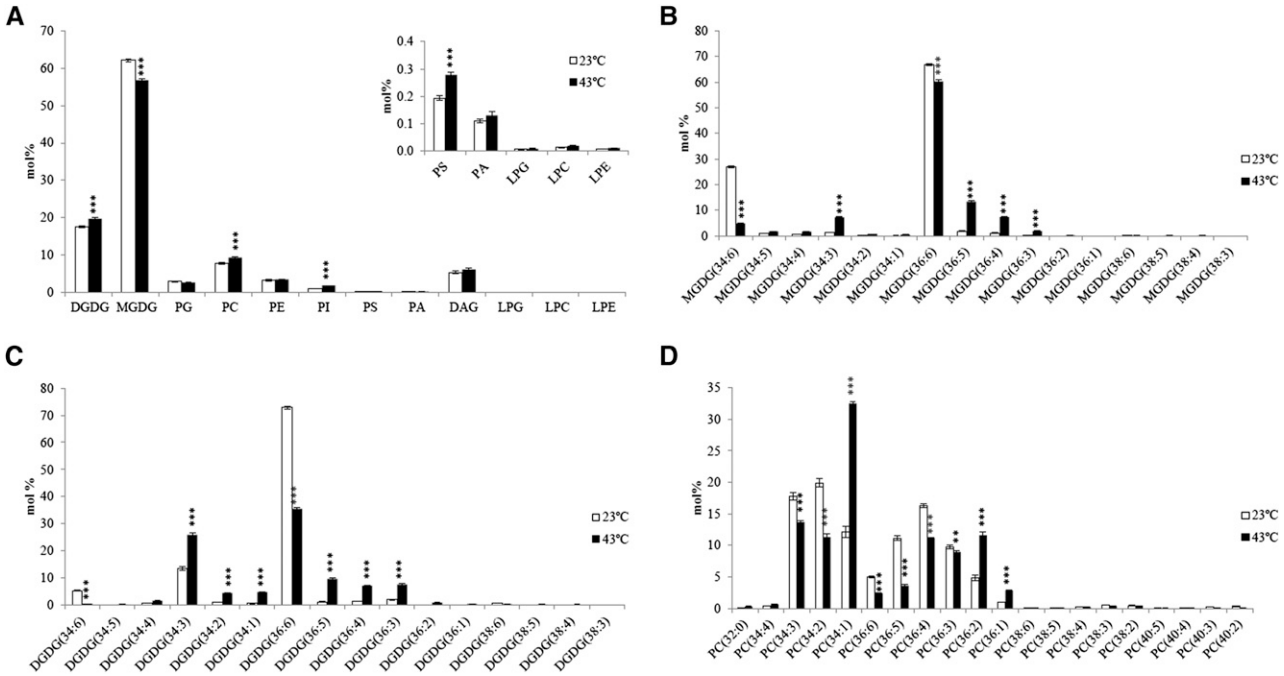

Figure 4. ESI-MS/MS Analysis of Glycerolipid Species in Leaves of in *A. lentiformis* Grown at 23°C and 43°C.

(A) Mol % of different lipid species in leaves of *A. lentiformis* grown at 23°C and 43°C.
(B) to **(D)** Molecular species of MGDG **(B)**, DGDG **(C)**, and PC **(D)** (mol %) in leaves of *A. lentiformis* grown at 23°C and 43°C. Detailed molecular compositions of all lipid species are available in Supplemental Data Set 1. Values are means ± SD (n = 5). *P < 0.05; **P < 0.01; ***P < 0.001.

et al., 2004). Hence, the repression of *FaTB* in *A. lentiformis* was consistent with an increased fatty acid efflux to the ER and an enhanced eukaryotic pathway.

The RNA-seq data set also yielded tantalizing hints on enzymatic components involved in trafficking of the ER glycerolipids to chloroplasts. Currently, the precise routes of DAG moieties originating from PC for chloroplast import remain uncertain (Benning, 2009). Likely candidates include PC-hydrolyzing phospholipase C that generates DAG and phospholipase D (PLD), which produces PA from PC (Welti et al., 2002; Peters et al., 2010; Reddy et al., 2010). In the light of enhanced contribution from the ER being observed in both *Arabidopsis* and *A. lentiformis* at high temperature, we note that the *NON SPECIFIC PHOSPHOLIPASE C4* (*NPC4*), which encodes a major PC-hydrolyzing phospholipase C (Nakamura et al., 2005; Peters et al., 2010; Reddy et al., 2010), was upregulated (1.9-fold) at 43°C. Two PLDs, *PLDgamma1* and *PLDzeta1*, by contrast, were downregulated 15.6- and 2.2-fold, respectively.

Triacylglycerols (TAGs), although representing <1% of total lipids in *Arabidopsis* leaf tissues, has been implicated in short-term glycerolipid intermediate provision during membrane lipid remodeling (James et al., 2010; Fan et al., 2013; Winichayakul et al., 2013). The breakdown of TAG in plants can be mediated by multiple TAG lipases (El-Kouhen et al., 2005; Eastmond, 2006). We found that in *A. lentiformis* the *MYZUS PERSICAE-INDUCED LIPASE1* (*MPL1*), which encodes a TAG lipase, was upregulated 43.7-fold at high temperature (Supplemental Data Set 4). Enzymes participating in TAG biosynthesis, including *DIACYLGLYCEROL ACYLTRANSFERASE3* (*DGAT3*) (2.1-fold), *LYSOPHOSPHATIDYL ACYLTRANSFERASE5* (5.0-fold), and *PHOSPHATIDYLCHOLINE:DIACYLGLYCEROL CHOLINEPHOSPHOTRANSFERASE* (2.9-fold), by contrast, were downregulated (Supplemental Data Set 4).

Temperature Treatment with *Arabidopsis* Lipid Mutants

Arabidopsis mutants with defined genetic lesions have served as powerful tools to study the relationship between lipid metabolism and temperature stress adaptation in plants (Falcone et al., 2004; Routaboul et al., 2012). The *fad5* (Hugly and Somerville, 1992) and *act1* (Kunst et al., 1988) mutants, each possessing a mutation that primarily effects the prokaryotic pathway, were indistinguishable from wild-type plants when raised under standard growth temperature, but they were more thermal tolerant and display higher growth rate at high temperature (Kunst et al., 1988; Falcone et al., 2004; Routaboul et al., 2012). In this study, *fad5* and *act1* were subjected to low-temperature treatment. Our experiments also included *gly1*, a glycerol-3-phosphate (G-3-P) dehydrogenase mutant, which is deficient in plastidic G-3-P provision and resulted in a reduced prokaryotic pathway to chloroplast lipid biosynthesis (Miquel et al., 1998). Significant reduction of 16:3 in leaves (Supplemental Table 3) confirmed the repression of the prokaryotic pathway in these mutants. The *fad5* mutant was previously shown to develop chlorosis in leaves at 5°C (Hugly and Somerville, 1992) and therefore was included in our experiments as a control for cold treatment. As shown in

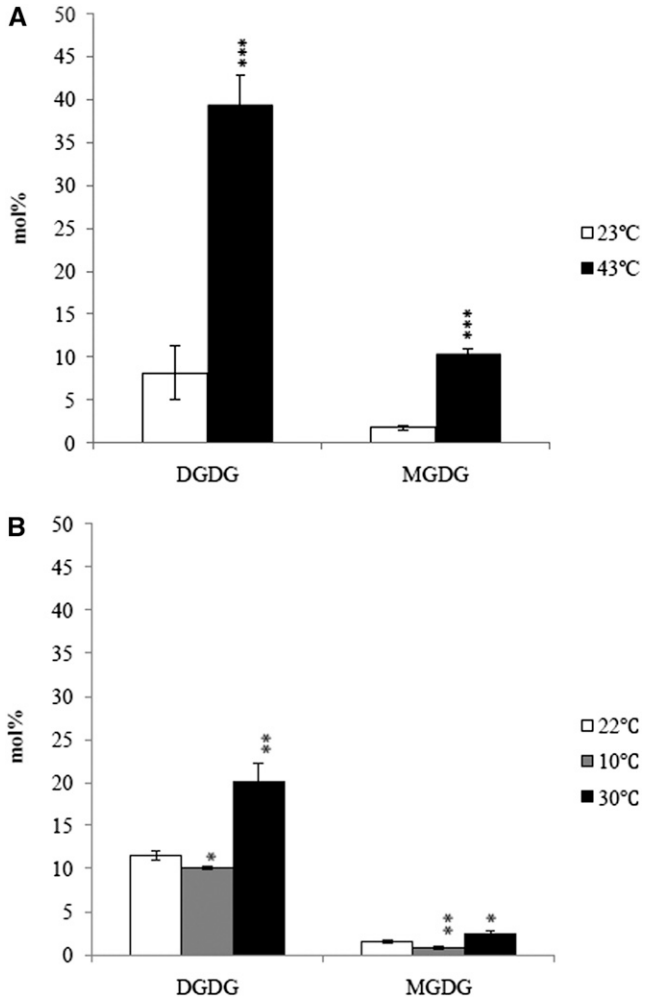

Figure 5. Distribution of *sn-1* 16:0 in MGDG and DGDG.

Mol % of 16:0 at the *sn-1* position in *A. lentiformis* **(A)** and *Arabidopsis* **(B)** was calculated based on stereo-specific analysis (*sn-2* position) and original fatty acid composition of individual lipids. Values are means ± SD (n = 3). *P < 0.05; **P < 0.01; ***P < 0.001.

Figure 6, similar to the *fad5* mutant, *gly1* developed chlorotic leaves after 3 weeks at 5°C. The *act1* mutant, despite being severely deficient in the major GPAT for the prokaryotic pathway (Kunst et al., 1988; Xu et al., 2006), did not exhibit noticeable chlorotic phenotype.

Lipid Pathway Sharing Pattern in Wheat Grown at 23°C and 4°C

Results from both *Arabidopsis* and *A. lentiformis* provided evidence of differential channeling of DAG moieties from the ER to chloroplasts. These changes influenced the molecular composition of MGDG and DGDG and also significantly affected the degree of desaturation in the chloroplast lipids. In 18:3 plants such as wheat, only the prokaryotic pathway contributes meaningfully to PG biosynthesis (Browse et al., 1986), while MGDG and DGDG are derived from the eukaryotic pathway. For this reason, we were interested in determining if the differential channeling of DAG moieties also takes place in 18:3 species and examined glycerolipid profile changes in wheat under low-temperature treatment. Wheat plants were grown at 23°C for 2 weeks (three-leaf stage), then shifted to 4°C for another 2 weeks (three-leaf stage). Total fatty acid analysis showed an increase in 18:3 and a decreased proportion of 16:0 and 18:2 at 4°C (Figure 7A). MGDG and SQDG were reduced, while PC, DGDG, and PE were increased (Figure 7B). Lipidomics analysis uncovered a similar trend of glycerolipid compositional changes (Supplemental Data Set 5). The proportion of PG was not changed, but it featured an increased C18 and a decreased C16 at the *sn-2* position (Figure 7C). Increase of C36 PG was also evident in the lipidomics data (Figure 8B), and the PG with *sn-2* C18 likely reflected biosynthesis of PG through the eukaryotic pathway. Overall, wheat plants produced higher percentage of phospholipids through the eukaryotic pathway at low temperature and decreased proportions of galactolipids (DGDG and MGDG) (Supplemental Table 4). Thus, in general agreement with results from *Arabidopsis* and *A. lentiformis*, there was a reduction of lipid channeling from the ER to the chloroplast at low temperature in wheat.

More importantly, a reduction of C34 DAG with a corresponding increase of C36 DAG was observed in wheat (Supplemental Figure 5), which suggested a differential channeling of DAG moieties for galactolipid biosynthesis in 18:3 plants as well. 2D-TLC analysis showed a reduction of 16:0 in DGDG (Figure 7D) at low temperature. An earlier study reported that in wheat more than 95 mol % of the *sn-2* in PC, PE, MGDG, and DGDG were of C18 fatty acids (Arunga and Morrison, 1971). Thus, the reduced 16:0 should be at the *sn-1* position of DGDG. In addition, the C16/C18 ratio in DGDG was decreased, which also suggested an increased partitioning of C18 fatty acids from the ER to the chloroplast (Supplemental Table 4). A reduction of C34:3(16:0/18:3) DGDG and an increased proportion of C36:6(18:3/18:3) DGDG was confirmed by lipidomics (Figure 8A). Thus, consistent with the data from 16:3 plants where high temperature promotes the channeling of C34 DAG (16:0/C18) and lower temperature stimulates the transport of C36 DAG (C18/C18), differential channeling of DAG moieties also occurs in 18:3 plants under temperature stress.

Figure 6. Temperature Effects on *Arabidopsis* Lipid Mutants with Compromised Prokaryotic Glycerolipid Pathway.

Mutants *gly1*, *fad5*, and *act1* along with wild-type control (ecotype Columbia) were grown at 22°C (10 d) and then shifted to 5°C for 3 weeks. Chlorotic leaves developed in *gly1* and *fad5* at 5°C, but not *act1*.

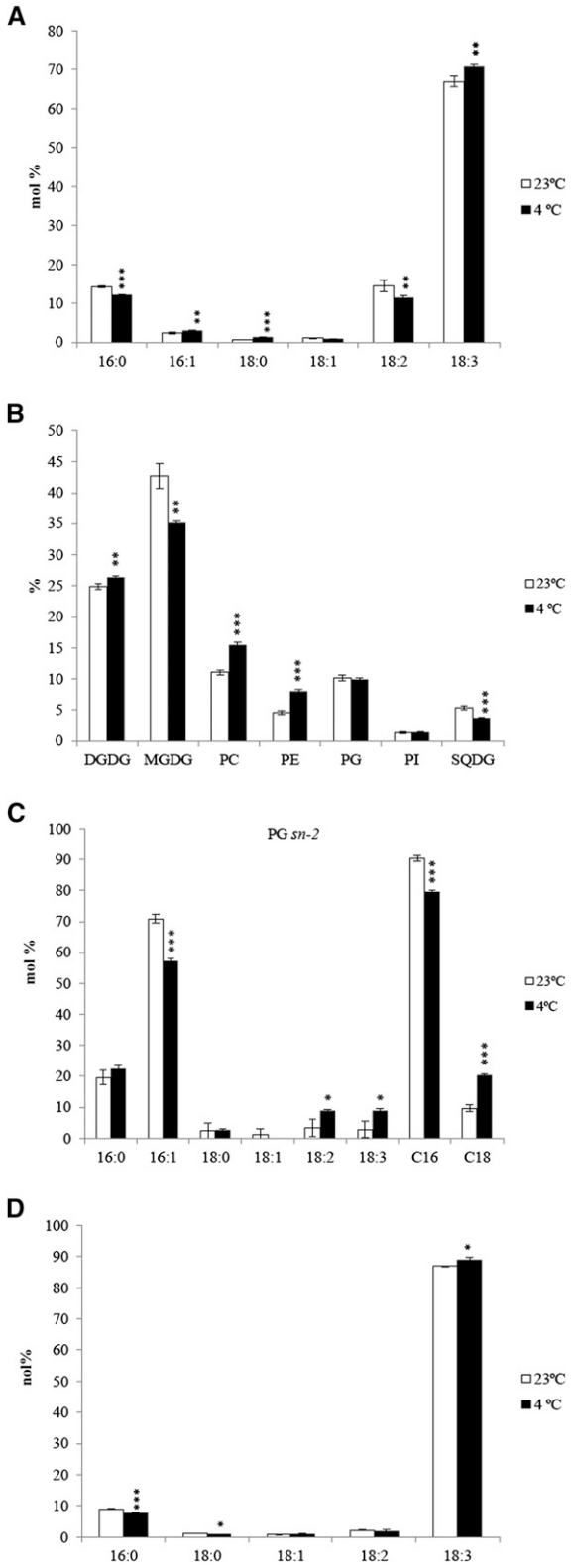

Figure 7. Lipid Analyses of Wheat Plants Grown at 23°C and 4°C.

(A) Total fatty acid composition analysis.

(B) Glycerolipid composition changes in response to low temperature.

(C) Stereo-specific analysis of fatty acid composition at the *sn-2* position of PG.

(D) Fatty acid composition in DGDG of wheat plants grown at 23°C and 4°C. C16 represents the sum of 16:l, 16:2, and 16:3; C18 represents the sum of 18:0, 18:1, 18:2, and 18:3. Values are means ± SD (n = 3). *P < 0.05; **P < 0.01; ***P < 0.001 (two-tailed Student's t test).

RNA-seq Analysis of Wheat Transcriptome

We further employed RNA-seq analysis to assess gene expression in wheat at 23°C and 4°C. Total RNA were extracted from control and cold-treated plants with three biological replicates for each growth condition. Quality filtered Illumina reads were mapped to the wheat genome survey sequence available at URGI (http://wheat-urgi.versailles.inra.fr/). A total of 135,920 transcripts were identified, of which the reference genome predicted 100,684 protein coding genes and 35,236 were newly identified transcripts (Supplemental Data Set 6). Coding sequence regions of predicted transcripts in the survey sequence and novel transcripts were annotated by BLASTx against the TAIR10 protein database using a cutoff of E^{-6}. Of the identified transcripts, 74,532 were considered as expressed (more than 50 reads per transcript across six samples) (Supplemental Data Set 7), and among the expressed transcripts, 51,230 were successfully annotated. The 1744 transcripts involved in lipid metabolism were categorized based on the lipid gene list (http://aralip.plantbiology.msu.edu) (Beisson et al., 2003; Li-Beisson et al., 2013) (Supplemental Data Set 8). Transcripts involved in fatty acid synthesis, glycerolipid synthesis, and TAG synthesis were specifically inspected (Supplemental Data Set 9).

Under low-temperature conditions, *FATTY ACID BIOSYNTHESIS2*, encoding a stearoyl-ACP desaturase converting 18:0-ACP to 18:1-ACP, was upregulated 2.3-fold. The transcript for another stearoyl-ACP desaturase, *DES2*, was also upregulated (97.3-fold). The upregulation of *ACYL-COA SYNTHETASE9* (3.0-fold), encoding a major acyl-CoA synthetase (Schnurr et al., 2002), suggested an increased fatty acid efflux from the chloroplast and a higher ER lipid biosynthesis. In the eukaryotic pathway, a homolog to the *Arabidopsis PAH1*, which encodes a phosphatidic acid phosphatase, was expressed at a much reduced level (2.7-fold). PAH is a negative regulator of de novo PC biosynthesis (Eastmond et al., 2010). Incidentally, transcripts involved in de novo PC and PE biosynthesis, including *AAPT1*, *AAPT2*, *PHOSPHORYLETHANOLAMINE CYTIDYLYLTRANSFERASE1*, *CHOLINE KINASE*, and *CHOLINE-PHOSPHATE CYTIDYLYLTRANSFERASE1*, were all detected at elevated levels. Together with the upregulated expression of *FAD2* (2.6-fold), the transcript profiles of these genes demonstrated a consistent pattern of increased ER pathway for PC and PE synthesis. In keeping with the increased proportion of DGDG, the transcripts encoding both MGD1 and DGD1, the two main synthases in MGDG and DGDG biosynthesis were upregulated, with *DGD1* at 4.4-fold and *MGD1* at 2.3-fold. Presumably, MGDG generated by MGD1 is subsequently converted to DGDG by the action of DGD1 (Kelly et al., 2003). Furthermore, *PLDzeta1*, which was downregulated at high temperature

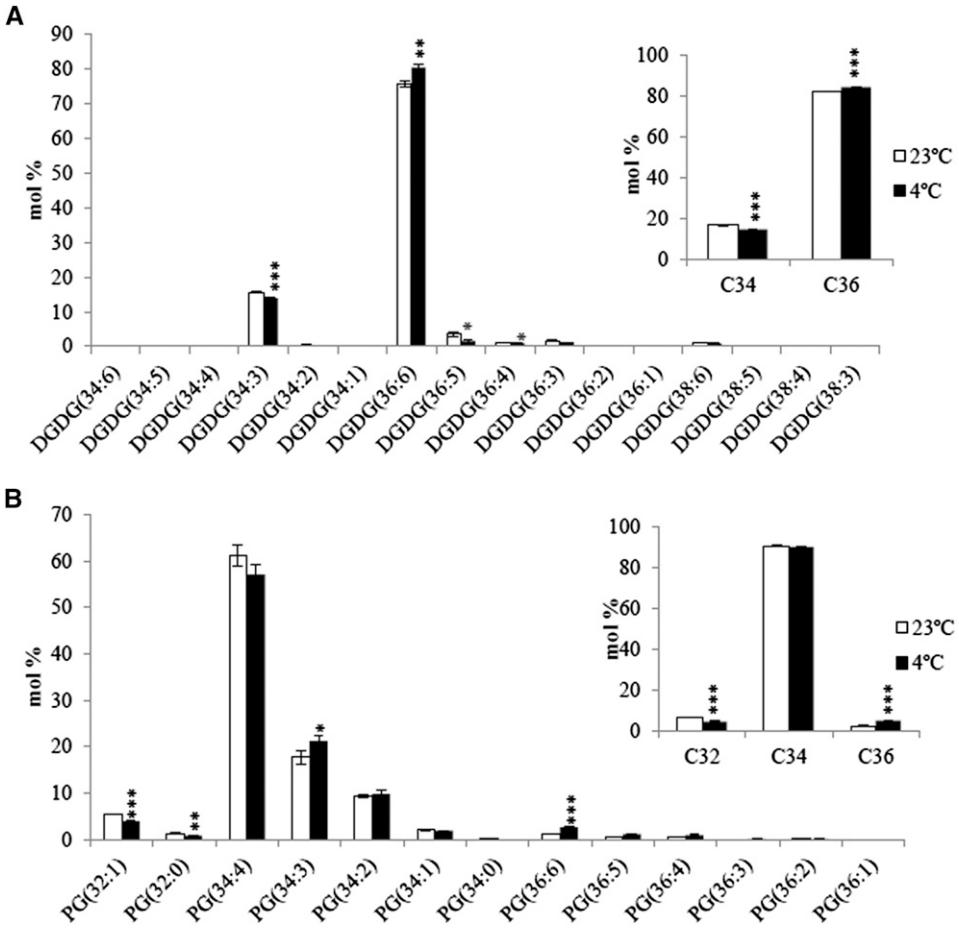

Figure 8. Lipidomics Analysis of Wheat.

Molecular composition of DGDG **(A)** and PG **(B)** in plants grown at 23°C and 4°C. Molecular compositions of all lipid species are available in Supplemental Data Set 5. C32 represents C16/C16 lipid molecules; C34 represents C16/C18 lipid molecules in DGDG or C16/C18 and C18/C16 in PG; C36 represents C18/C18 lipid molecules. Values are means ± SD (n = 3). *P < 0.05; **P < 0.01; ***P < 0.001(two-tailed Student's t test).

in *A. lentiformis*, was upregulated 2.9-fold at low temperature in wheat.

Accumulation of TAGs in leaves has been reported in *Arabidopsis* under freezing temperature and involves *SENSITIVE TO FREEZING2* (*SFR2*), which encodes a galactolipid remodeling enzyme contributing to TAG accumulation (Moellering et al., 2010). We did not detect a change in *SFR2* transcript level in wheat (Supplemental Data Set 9). However, studies have shown that SFR2 activity is primarily regulated at the posttranslational level during freezing tolerance (Moellering et al., 2010). Five genes potentially involved in TAG breakdown including *LIPASE1* (El-Kouhen et al., 2005), *SUGAR-DEPENDENT1* (Eastmond, 2006), *MPL1* (El-Kouhen et al., 2005), and two putative *TAGL*s were downregulated more than 2-fold. The *ACYL-COA OXIDASE2* (Pinfield-Wells et al., 2005) of β-oxidation pathway was also downregulated (2.6-fold). By contrast, *DGAT1* (Zou et al., 1999; Katavic et al., 1995), a key component of TAG biosynthesis, was upregulated 2.5-fold. Interestingly, genes required for the formation of oil bodies were also induced, including *CALEOSIN*s (*CLO1*, 18.3-fold; *CLO3*, 20.2-fold), *STEROLEOSIN*s (*HSD1*, 2.7-fold), and *OLEOSIN*s (*OBO*, 5.3-fold) (Supplemental Data Set 9).

DISCUSSION

In this study, we investigated the dynamics of glycerolipid pathway coordination under different temperatures in *Arabidopsis*, *A. lentiformis*, and wheat. We propose a model, presented in Figure 9, outlining major pathway adjustments in response to temperature changes and key metabolic junctures involved in this process. This model emphasizes the notion that glycerolipid pathway adjustment between the chloroplast and cytosolic compartment is a general framework to modulate lipid composition under temperature stress. This model helps to explain why some of the desaturase genes are suppressed under low temperature conditions when a higher degree of lipid desaturation is achieved. Even though desaturases are the enzymes mediating the formation of double bonds in fatty acyl moieties, it is the glycerolipids in the membrane systems that serve as the necessary substrate and provide the proper metabolic context for

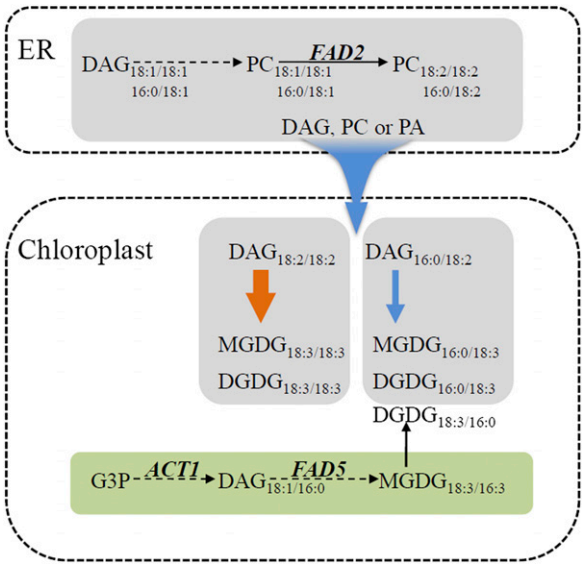

Figure 9. Glycerolipid Pathway Coordination in Response to Growth Temperature.

Glycerolipid species derived from the eukaryotic pathway are shown in gray (*sn-1/sn-2*, C18/C18 or C16/C18); glycerolipids originating from the prokaryotic pathway are in green (*sn-1/sn-2*, C18/C16). Blue arrows denote trends associated with increase in growth temperature, whereas the orange arrow indicates changes associated with decrease in growth temperature. Higher temperature suppresses the prokaryotic pathway and promotes lipid trafficking from the ER to chloroplast. DAG moieties of C18/C18 and 16:0/C18 derived from the ER are differentially transported to the chloroplast for the biosynthesis of MGDG and DGDG. Higher temperature induces the trafficking of DAG (16:0/C18), while lower temperature stimulates the channeling of DAG (C18/C18). *FAD2*, *FAD5*, and *ACT1* are key genes influencing fatty acid flux sharing between the two glycerolipid pathways.

desaturases to act upon. In comparison to direct regulation of desaturases, glycerolipid pathway balancing offers a system-wide flexibility. At the same time, this regulatory regime serves to stabilize lipid metabolic network against drastic and transitory changes, thereby ensuring biological robustness under temperature fluctuations.

Pathway Adjustment Underlying Glycerolipid Compositional Changes at High and Low Temperature

Low-temperature-induced MGDG biosynthesis was previously suggested as conferring plant performance advantage because desaturation on MGDG occurred more quickly at low temperature (Johnson and Williams, 1989). MGDG could be biosynthesized from either the prokaryotic or the eukaryotic pathways. In this study, we showed that in *Arabidopsis* low-temperature-induced MGDG biosynthesis originated primarily from an enhanced prokaryotic pathway, while high temperature induced an increased DGDG through redirection of acyl channeling from the eukaryotic pathway. Glycerolipid compositional changes in *Arabidopsis* at either high or low temperature were largely attributable to a rebalancing of the two pathways.

A. lentiformis represents an extreme case of lipid profile changes under thermo-stress. Lipidomics analysis showed that the increased DGDG and MGDG were mostly derived from eukaryotic pathway. Unlike typical 18:3 plants wherein galactolipids are entirely derived from the eukaryotic pathway (Browse et al., 1986), the repressed prokaryotic pathway in *A. lentiformis* under high temperature still produced some portion of chloroplast galactolipids. Hence, as far as enzymatic network of lipid metabolism is concerned, *A. lentiformis* is still a 16:3 plant at 43°C, but the severely suppressed prokaryotic pathway effectively converts its lipid profile from 16:3 to 18:3.

In wheat, there was reduced glycerolipid channeling from the ER to chloroplast and the proportions of phospholipids in the ER were increased when grown at 4°C. Different from 16:3 plants, wheat under low temperature had a decreased proportion of MGDG and increased DGDG. Labeling studies have shown that in *B. napus*, ER-derived MGDG is desaturated at a much slower rate than the ER-derived DGDG (Johnson and Williams, 1989). Assuming that it is also true in wheat that the desaturation of ER-derived DGDG is faster than that of MGDG, an increase of DGDG at low temperature in wheat would be beneficial for efficient desaturation of overall chloroplast galactolipids.

Differential Channeling of DAG Moieties from the ER to Chloroplasts under Suboptimal Growth Temperatures

PC or PC-derived lipids (DAG, PA, and/or *lyso*-PC) are likely precursors, directly or indirectly, to be trafficked to chloroplast for galactolipid biosynthesis (Kelly et al., 2003; Benning, 2009). Labeling experiments in *Arabidopsis* have demonstrated that PC with a DAG moiety of C18/C18 is preferentially transported for MGDG and DGDG biosynthesis, while C16 fatty acids are retained in PC (Browse et al., 1986; Miquel and Browse, 1992). This study uncovered evidence of a preferential channeling of C34 DAG moieties from the ER to chloroplast under conditions of high temperature in *Arabidopsis* and *A. lentiformis.* In wheat, we also detected decreased C34 DGDG and increased C36 DGDG at low temperature. A boosted channeling of C34 DAG moieties from the ER to chloroplast for DGDG biosynthesis has previously been observed under phosphate-deprived condition (Härtel et al., 2000), while an export of C36 DAG moieties from chloroplast for phospholipid biosynthesis in the ER was noted during dehydration in plants (Gasulla et al., 2013). Thus, differential channeling of C34 DAG and C36 DAG moieties between the ER and chloroplast could be an important mechanism of plant adaptation to environmental stress. In the context of temperature stress, an increase of C34 (16:0/18C) DAG moiety for galactolipid biosynthesis might be advantageous for growth under high temperature because in comparison to C36:6 (18:3/18:3) galactolipids, C34 MGDG and DGDG only permit lower degrees of unsaturation (16:0/18:3).

Key Factors Influencing Glycerolipid Pathway Adjustment under Temperature Stress

Our results show that glycerolipid pathway adjustment involved enzymatic components beyond those directly participating in the fatty acid assembly process. The transcript level of *FAD5*, a fatty acyl desaturase utilizing MGDG as substrate, was positively

correlated with contributions of the prokaryotic pathway. It was previously reported that disruption of *FAD5* in *Arabidopsis* resulted in a compromised prokaryotic pathway (Hugly and Somerville, 1992). In *Arabidopsis* transgenic lines of augmented G-3-P content, an induction of *FAD5* coincided with an enhanced prokaryotic pathway (Shen et al., 2010). Interestingly, in wheat, where MGDG or DGDG are produced through the eukaryotic pathway, *FAD5* homologs were conspicuously absent from its genome. Neither were homologs of *FAD5* identifiable in the genome of another 18:3 plant, rice (*Oryza sativa*) (Heilmann et al., 2004). These findings suggest that FAD5 has a significant role to play in relation to the contribution of prokaryotic pathway.

We also find that expression of *FAD2* was positively associated with contributions of the eukaryotic pathway. *FAD2* encodes the major desaturase mediating the desaturation of 18:1 to 18:2 in PC and possibly other phospholipids (Miquel et al., 1993) of the eukaryotic pathway. Disruption of *FAD2* in *Arabidopsis* has been shown to result in reduced lipid channeling from the ER to chloroplast for both MGDG and DGDG biosynthesis (Miquel and Browse, 1992). In this study, transcript of *FAD2* in *Arabidopsis* exhibited a pattern of increased expression from 10°C to 30°C, when the relative contribution of the eukaryotic pathway was higher. In *A. lentiformis*, *FAD2* transcript was also induced at high temperature when the eukaryotic pathway predominated. In wheat, *FAD2* was induced at low temperature and also correlated with the enhanced eukaryotic pathway. In developing seeds, an induction of *FAD2-1* and *FAD2-2* expression in soybean (*Glycine max*) at high temperature has been reported previously (Heppard et al., 1996), but that was rationalized in the context of post-transcriptional regulation of enhanced degradation of the soybean FAD2-1 (Tang et al., 2005). However, it is also possible that the induction of *FAD2* was associated with a higher lipid pathway activity through the eukaryotic pathway in developing seeds.

Our study also revealed clues with regard to how differential channeling of DAG moieties was brought about. At least two possible routes exist for PC-derived DAG and/or PA generation: (1) the nonspecific PLCs (NPCs) and (2) the PLDs (Vergnolle et al., 2005; Peters et al., 2010). In vivo substrate analysis in *Chlamydomonas moewusii* showed that PLDs have preferences toward C18/C18 phospholipids, while activation of PLC resulted in increased PA of C16:0/C18:1 and PA C16:0/C18:3 (Welti et al., 2002; Arisz et al., 2003). In *Arabidopsis*, *NPC4* and *NPC5* were shown to play important roles in hydrolyzing PC to generate DAG (Nakamura et al., 2005; Peters et al., 2010; Reddy et al., 2010). Conversion of PC to PA was proposed to be catalyzed by PLDzeta1 and PLDzeta2 (Cruz-Ramírez et al., 2006; Li et al., 2006). At 43°C, we observed an induction of *NPC*s and concomitant repression of *PLD*s in *A. lentiformis*. Under low temperature, *PLDzeta1* was upregulated in wheat. The substrate specificities of these enzymes in *A. lentiformis* and wheat are not yet clear. Nonetheless, an increase of C34 PA and a reduction of C36 PA were observed in *A. lentiformis* at high temperature. Furthermore, decreased C34 DAG and increased C36 DAG were detected in wheat at low temperature. Hence, we speculate that high-temperature-induced NPC allows elevated production of C34 DAG (16:0/C18), while lower temperature stimulates the PLD pathway to generate C36 DAG (C18/C18) for galactolipid biosynthesis. More efforts are required to validate this supposition.

Physiological Relevance of Glycerolipid Pathway Adjustment in Temperature Adaptation

A series of desaturase mutants in *Arabidopsis* have been investigated under temperature stress, including *fad2* (Miquel et al., 1993), *fad5* (Hugly and Somerville, 1992), *fad6* (Hugly et al., 1989), and *fad3 fad7 fad8* triple mutants (McConn and Browse, 1996). These mutants, indistinguishable from wild-type plants when grown at 22°C, all displayed symptoms of damage at low temperature. Clearly, the degree of membrane unsaturation, disturbed in these desaturase mutants, is one determining factor in adaptation to temperature stress. Our results in this study highlight the significance of changes in membrane lipid compositions, which were also observed in these mutants (Hugly et al., 1989; Hugly and Somerville, 1992; Miquel et al., 1993; McConn and Browse, 1996). We showed that growth of *gly1* was compromised under low temperature, even though its DBI was very close to the wild type (Supplemental Table 3). The *act1* mutant, like *fad5* (Routaboul et al., 2012), was more thermal tolerant (Kunst et al., 1989), but its DBI resembles that of the wild type at either 17°C or 36°C (Falcone et al., 2004). Unlike *fad5*, *act1* displays no apparent performance disadvantage under low temperature (Kunst et al., 1989; this study). Hence, glycerolipid composition and the degree of fatty acid desaturation are two major factors underpinning membrane performance during temperature stress. Glycerolipid pathway readjustment provides a system-wide regulation influencing both of them.

METHODS

Plant Materials and Growth Conditions

Plants were grown in growth chambers (Conviron) in Sunshine Mix#3/LG3 soil (Sun Gro Horticulture). Three growth chambers with a 16-h-light (~120 μmol m^{-2} s^{-1})/8-h-dark regime were employed for the experiments with *Arabidopsis thaliana* (ecotype Columbia-0). Plants were grown at 22/17°C (day/night temperature) for 1 week after germination and then 1/3 were moved to 10/8°C (low temperature) and 1/3 were moved to 30/28°C (high temperature) for another 3 weeks, hereafter referred to as 22°C, 10°C, and 30°C, respectively. Plants grown at 22°C for 4 weeks were used as control. For each treatment, leaves from at least three independent biological replicates (plants were grown at least three times in the same chamber under the same growth conditions) of 4-week-old plants were collected for biochemical and transcript analysis.

Atriplex lentiformis seeds (Stover Seed Company) were germinated and grown in two growth chambers under either 23/18°C or 43/30°C day/night temperature regime with a 16-h photoperiod and light intensity of 120 μmol m^{-2} s^{-1} (Pearcy, 1978), respectively. Hereafter, these treatments are referred to as 23°C and 43°C. Leaves were harvested from at least three biological replicates (plants were grown at least three times in the same chamber) of 8-week-old plants grown under each treatment for biochemical and transcriptomic analysis.

Wheat (*Triticum aestivum* cv Manitou) was grown in soil at 23°C for 2 weeks (three-leaf stage) after germination, and then half of plants were moved to 4°C for cold treatment for another 2 weeks (three-leaf stage). Light intensity in both chambers was ~120 μmol m^{-2} s^{-1}. Plants grown at 23°C for 2 weeks were used as control. Three biological replicates (plants were grown in the same chamber three times) of aboveground plant material were harvested for biochemical and transcriptomic analysis for each treatment temperature. Leaf samples were frozen in liquid N_2 immediately after harvesting and stored at −80°C.

Arabidopsis mutants (*fad5*, CS206; *act1*, CS200; *gly1*, Salk_111786c) were ordered from ABRC and have been previously described (Kunst et al., 1988; Hugly and Somerville, 1992; Miquel et al., 1998). For this experiment, two growth chambers with a 16-h-light (~120 μmol m^{-2} s^{-1})/8-h-dark regime were employed. Plants were grown in soil at 22°C for 1 week after germination. Half of the plants were then shifted to a 5°C growth chamber for low temperature, while the other half of plants were continuing grown at 22°C until 10 d after germination. Plants were grown three times in the same chamber. For cold treatment, 5°C was selected as the *fad5* mutants have shown chlorosis (Hugly and Somerville, 1992). For low-temperature treatment, 3-week-old rosette leaves from three independent biological replicates were collected for biochemical analysis.

Fatty Acid and Lipid Analysis

Tissue samples (10 to 50 mg) for total fatty acid analysis were placed in a Teflon-lined screw cap glass tube that was prerinsed with 2 mL dichloromethane. One milliliter of 5% (v/v) sulfuric acid in methanol, 20 μL of 0.2% butylated hydroxy toluene in methanol, and 300 μL toluene were added as cosolvents. After 2 h heating at 80°C, the tubes were cooled and 1 mL of 0.9% (w/v) NaCl and 0.35 mL hexane were added. The tubes were vortexed vigorously and centrifuged at 1500*g* for 3 min. The upper phase (organic phase) was transferred to a new tube and dried under nitrogen steam. After redissolving in hexane, the fatty acid methyl esters were analyzed by gas chromatography on a DB-23 column (Shen et al., 2010). An estimation of the membrane total unsaturation level by double bond index was calculated from mol % values of each fatty acid using the formula: DBI = [∑(number of double bonds ± mol % of fatty acid)]/100 (Falcone et al., 2004).

Lipid extractions followed the methods described by Miquel and Browse (1992) and Shen et al. (2010). Polar lipids were extracted from 0.5 g harvested plant tissues. All samples were frozen rapidly by immersion in liquid N_2 and ground into powder under liquid N_2 with a mortar and pestle. The extracts were dissolved in 6 mL chloroform/methanol/formic acid (10:10:1, v/v/v) and transferred into a glass tube with a Teflon-lined screw cap. The extracts were centrifuged at 1000*g* for 6 min, and the upper phase was saved in a new tube. The extracts were then reextracted with 2 mL chloroform/methanol/formic acid (5:5:1, v/v/v) and combined with the first extraction after centrifuging. The mixture was washed with 3 mL 0.2 M H_3PO_4 and centrifuged for 8 min at 1000*g*. Lipids were recovered in the organic phase and dried under nitrogen steam. After redissolving in chloroform, total lipids were separated by 2D-TLC using a two-solvent system; chloroform/methanol/ 50% ammonia hydroxide (65:25:2, v/v/v) solvent for one direction and then chloroform/methanol/acetic acid/water (85:15:10:3, v/v/v/v) solvent for second direction. TLC plates were sprayed with 0.05% primulin in 80% acetone and lipids were visualized under UV light. Individual lipids were scraped off TLC plates and transferred into a glass tube with a Teflon-lined screw cap. Transmethylation of lipids was performed by adding 2 mL 3 N methanolic HCl and heating at 80°C for 2 h. Fatty acid methyl derivatives of each lipid were extracted with hexane and determined by gas chromatographic analysis.

Stereo-Specific Analysis

Stereo-specific analysis was performed according to Shen et al. (2010). Individual lipid species were separated by 2D-TLC and then eluted from TLC plates by chloroform and methanol (2:1, v/v). Each lipid was then dissolved in 1 mL 40 mM Tris-HCl buffer, pH 7.2, and 0.05% Triton X-100 containing 50 mM H_3BO_3. The reaction was started by adding 3000 units *Rhizopus arrhizus* lipase (Sigma-Aldrich) suspended in the same buffer. The mixture was incubated at 37°C for 20 to 60 min. Lipids were then extracted with 3.8 mL chloroform and methanol (2:1, v/v) and 1 mL 0.15 M acetic acid. The organic phase was collected and separated on TLC plates with chloroform/methanol/acetic acid/water (85:15:10:3, v/v/v/v). The *lyso*-lipids containing fatty acids at the *sn-2* position were scraped off TLC plates for gas chromatographic analysis after transmethylation. Fatty acid composition at *sn-1* position was calculated based on the fatty acid compositions of the original diacyl lipid and the *lyso*-lipid.

Lipidomic Analysis

Lipid extractions for lipidomics analysis were performed according to the protocol from the Kansas Lipidomics Research Center (http://www.k-state.edu/lipid/lipidomics). Briefly, tissues from *A. lentiformis* and wheat plants were heated in 2 mL isopropanol with 0.01% butylated hydroxy-toluene at 75°C for 10 min to inactivate the lipases. Chloroform and methanol (2:1, v/v) were added for extraction. After several extractions, the combined extracts were washed with 1 M KCl to remove proteins and carbohydrates. The chloroform phase was removed and dried under a nitrogen stream. Lipid extracts were dissolved in chloroform for lipidomic analysis. ESI-MS/MS analysis was performed at the Kansas Lipidomic Research Center (Welti et al., 2002). The data for each lipid molecular species are presented as mol % of the total lipids analyzed. Statistically significant differences were calculated by two-tailed Student's *t* test.

Real-Time qRT-PCR Analyses

Total RNA was extracted from the leaves of *Arabidopsis* grown at 10°C, 22°C, and 30°C using the Plant RNeasy Mini kit (Qiagen). RNA quality and quantity were determined by spectrophotometry at 260 and 280 nm using the NanoDrop 2000 (Thermo-Scientific). cDNA was generated using 1 μg total RNA using QuantiTect Reverse Transcription kit (Qiagen). Specific primers (Tm, 57°C to 63°C) were designed to generate PCR products between 75 and 130 bp. Primer specificity was checked with BLASTn searches against TAIR10 transcripts (http://www.arabidopsis.org/) as well as by monitoring melt curve using the ABI StepOne Real-time PCR systems (Applied Biosystems). *ACTIN2* (*At3g18780*) was used as an endogenous control for standardization (Huang et al., 2007). Real-time qRT-PCR was performed with Power SYBR Green PCR Master Mix (Applied Biosystems), and amplification was monitored with StepOne real-time PCR systems. A standard thermal profile was used for all PCRs: 50°C for 2 min and 95°C for 10 min, followed by 40 cycles of 95°C for 15 s, 57°C for 30 s, and 72°C for 30 s. qRT-PCR was performed with three biological replicates for each gene. For each biological replicate, three technical replicates were included for each PCR reaction. In each technical replicate, the results from control plants (22°C) were normalized to one using StepOne software 2.0 (Applied Biosystems), while the relative expression values from plants grown at 10°C and 30°C were presented as fold change against plants grown at 22°C using the comparative Ct (ΔΔCt) method. Each biological replicate represents average values of three technical replicates. Statistically significant differences (two-tailed Student's *t* test) were calculated from three biological replicates between temperature treatments (10°C and 30°C) to standard growth condition (22°C), respectively. The primers used for qRT-PCR are listed in Supplemental Table 5.

RNA Sequencing and Data Analysis

Total RNA was extracted from eight samples (four biological replicates for each growth condition) of *A. lentiformis* leaf tissues grown at 23°C and 43°C using the Agilent Plant RNA isolation kit (Agilent Technologies). Eight cDNA libraries were constructed from leaves with four biological replicates for each growth condition using the TruSeq RNA Sample Preparation Kit v2 (Illumina). Sequencing reactions were conducted on the Illumina HiSeq2000 at the National Research Council, Aquatic and Crop Resource Development (ACRD)-Saskatoon, Canada. Paired-end sequencing was performed on a 200-bp insert library, generating 2 × 101-bp reads. After removing sequencing adapters and trimming low-quality reads with

Btrim (Kong, 2011; default settings), repeat masking was performed by removing reads with hits against the TIGR Plant Repeats Database (Ouyang and Buell, 2004) using Bowtie2 with maximum fragment length of 1000 nucleotides (Langmead and Salzberg, 2012). Reads were then assembled into contigs using Trinity (version 2013-02-25) using default parameters following the protocol documented by Haas et al. (2013) and Grabherr et al. (2011). The contigs produced by Trinity were then further assembled by CAP3 (Huang and Madan, 1999) to reduce redundancy. Illumina reads were then mapped back onto the CAP3 contigs using the alignReadsl.pl script with Trinity and transcript abundances estimated with RSEM via the run_RSEM_align_n_estimate.pl script, also included with Trinity. Transcripts with at least 50 aligned reads across the eight samples were defined as expressed to eliminate extreme low expression values and used for differential expression analysis. Of the unique transcripts, 46,492 met the criteria and used for further analysis (Supplemental Data Set 2). Normalized transcript expression levels were estimated according to the transcript features (length, depth of sequencing, and reads) and sample size in units of fragments per kilobase of exon per million fragments (Robinson et al., 2010). For each transcript, the mean $\log_2$ fold change and corresponding P value were calculated using the edgeR package (Robinson et al., 2010) from average between four biological replicates of each experimental condition. False discovery rate correction (Benjamini and Hochberg, 1995) was applied to account for testing of multiple transcripts. Transcripts were considered differentially regulated if the P value was <0.01 and the fold change in expression level was greater than four. Putative functions of all transcripts were assigned using BLASTx searches (E-value cutoff of 10^{-6}) against *Arabidopsis* TAIR10 protein database for downstream analysis. The assembled transcripts were further characterized and categorized for lipid metabolism genes (Supplemental Data Set 3). Transcripts involved in glycerolipid pathways were extracted and specifically inspected (Supplemental Data Set 4).

For wheat, six cDNA libraries were constructed from total RNA with three biological replicates for each growth temperature using the TruSeq RNA Sample Preparation Kit v2 (Illumina). Paired-end sequencing was conducted on the Illumina HiSeq2500, generating 101-nucleotide reads, at the National Research Council, ACRD-Saskatoon, Canada. Raw reads were trimmed to remove adapters and low quality reads using Trimmomatic (Bolger et al., 2014), with parameters ILLUMINACLIP:truseq_adapters.fasta:2:30:10 LEADING:17 SLIDINGWINDOW:5:15 MINLEN:50. The filtered reads from six libraries were mapped to the wheat genome survey sequence obtained from URGI (http://wheat-urgi.versailles.inra.fr/) (International Wheat Genome Sequencing Consortium, 2014) using STAR (Dobin et al., 2013) with parameters: –outFilterMultimapScoreRange 0, –alignIntronMax 25000, –outFilterMismatchNmax 4, –outFilterMatchNminOverLread 0.9. Transcript identification was then performed with Cufflinks in GTF guided mode and followed by Cuffmerge and Cuffdiff for differential expression analysis (Trapnell et al., 2012). For the annotation, coding sequence regions of each gene in the wheat reference genome as well as the novel transcripts were compared (BLASTx) against the TAIR10 protein database using a cutoff of E^{-6}. Read counts per transcript were estimated using HTseq (Anders et al., 2014), and transcripts with fewer than 50 reads aligned across six samples were excluded to eliminate the extreme low expression transcripts (Supplemental Data Set 7). Transcripts involved in lipid metabolism (Supplemental Data Set 8) and glycerolipid pathways (Supplemental Data Set 9) were extracted.

Accession Numbers

Sequence data from this article can be found in the Arabidopsis Genome Initiative database under accession numbers listed in Supplemental Table 5 and Supplemental Data Sets 2 and 6. The raw RNA-seq data and normalized expression data of the *A. lentiformis* transcriptome are deposited to National Center for Biotechnology Information Gene Expression Omnibus under accession number GSE52913. The raw RNA-seq data for wheat were deposited in the Gene Expression Omnibus under accession number GSE58805.

Supplemental Data

Supplemental Figure 1. Total Fatty Acid Composition in Leaves of *Arabidopsis* Grown at 10, 22, and 30°C.

Supplemental Figure 2. Double Bond Index Values of Individual Lipid Species of *Arabidopsis* Grown at 10, 22, and 30°C.

Supplemental Figure 3. Leaf Fatty Acid Compositions of *A. lentiformis* Grown at 23°C and 43°C.

Supplemental Figure 4. Changes in PA and DAG Subpools in *A. lentiformis* Grown at 43°C and 23°C.

Supplemental Figure 5. Changes in PA and DAG Subpools in Wheat Grown at 4°C and 23°C.

Supplemental Table 1. Leaf Glycerolipid Composition of *Arabidopsis* Grown at 10, 22, and 30°C.

Supplemental Table 2. Leaf Glycerolipid Compositions of *A. lentiformis* Grown at 23°C and 43°C.

Supplemental Table 3. Fatty Acid Composition of Plants Grown at 22°C (10 d) and after Exposure to 5°C for 3 Weeks.

Supplemental Table 4. Leaf Glycerolipid Composition of Wheat at 23°C and 4°C.

Supplemental Table 5. Primers Pairs Used in This Study.

Supplemental Data Set 1. Lipid Species *A. lentiformis* Leaves Grown at 23°C and 43°C as Assessed by ESI-MS/MS.

Supplemental Data Set 2. Transcriptomics Analysis of *A. lentiformis* Grown at 43°C and 23°C.

Supplemental Data Set 3. Differences in Transcript Levels of Genes Involved in Lipid Metabolism in *A. lentiformis* Grown at 43°C Compared with 23°C.

Supplemental Data Set 4. Differences in Transcript Level of Genes in Glycerolipid Pathways and TAG Biosynthesis in *A. lentiformis* Grown at 43°C Compared with 23°C.

Supplemental Data Set 5. Lipid Species in Wheat Leaves at 23°C and 4°C as Revealed by ESI-MS/MS.

Supplemental Data Set 6. Transcriptomics Analysis of Wheat Grown at 23°C and 4°C.

Supplemental Data Set 7. Differential Gene Expression Analysis of Wheat Grown at 23°C and 4°C.

Supplemental Data Set 8. Relative Expression of Transcripts Involved in Lipid Metabolism in Wheat Grown at 4°C Compared with 23°C.

Supplemental Data Set 9. Relative Expression of Transcripts Involved in Glycerolipid Pathways and TAG Biosynthesis in Wheat Grown at 4°C Compared with 23°C.

ACKNOWLEDGMENTS

We thank Darrin Klassen from ACRD-Saskatoon for assistance with Illumina sequencing and Youlian Pan from Information and Communications Technologies, National Research Council for data analysis. We thank J. Allan Feurtado, Lipu Wang, Patricia Vrinten, and Mark Smith from ACRD-Saskatoon for critical reading of the article. We also thank Mary Roth and Ruth Welti of the Kansas Lipidomics Research Center for lipidomic analysis. This research was supported in part by the Canadian

Wheat Alliance program. This research is a National Research Council Canada Publication (55620).

AUTHOR CONTRIBUTIONS

Q.L. and J.Z. designed the experiments. Q.L. performed the experiments. Q.L., Q.Z., W.S., and D.C. analyzed the data. Q.L., B.F., Y.W., and J.Z. wrote the article.

Received November 17, 2014; revised December 11, 2014; accepted December 16, 2014; published January 6, 2015.

REFERENCES

Anders, S., Pyl, P.T., and Huber, W. (2014). HTSeq: A Python framework to work with high-throughput sequencing data. Bioinformatics **pii:** btu638.

Arisz, S.A., Valianpour, F., van Gennip, A.H., and Munnik, T. (2003). Substrate preference of stress-activated phospholipase D in Chlamydomonas and its contribution to PA formation. Plant J. **34:** 595–604.

Arunga, R.O., and Morrison, W.R. (1971). The structural analysis of wheat flour glycerolipids. Lipids **6:** 768–776.

Beisson, F., et al. (2003). Arabidopsis genes involved in acyl lipid metabolism. A 2003 census of the candidates, a study of the distribution of expressed sequence tags in organs, and a web-based database. Plant Physiol. **132:** 681–697.

Benjamini, Y., and Hochberg, Y. (1995). Controlling the false discovery rate: a practical and powerful approach to multiple testing. J. R. Stat. Soc. B **57:** 289–300.

Benning, C. (2009). Mechanisms of lipid transport involved in organelle biogenesis in plant cells. Annu. Rev. Cell Dev. Biol. **25:** 71–91.

Benning, C., Xu, C., and Awai, K. (2006). Non-vesicular and vesicular lipid trafficking involving plastids. Curr. Opin. Plant Biol. **9:** 241–247.

Bolger, A.M., Lohse, M., and Usadel, B. (2014). Trimmomatic: a flexible trimmer for Illumina sequence data. Bioinformatics **30:** 2114–2120.

Bonaventure, G., Bao, X., Ohlrogge, J., and Pollard, M. (2004). Metabolic responses to the reduction in palmitate caused by disruption of the FATB gene in Arabidopsis. Plant Physiol. **135:** 1269–1279.

Brockman, J.A., Norman, H.A., and Hilderbrand, D.F. (1990). Effects of temperature, light and a chemical modulator on linolenate biosyntheis in mutant and wild type *Arabidopsis* calli. Phytochemistry **29:** 1447–1453.

Browse, J., Warwick, N., Somerville, C.R., and Slack, C.R. (1986). Fluxes through the prokaryotic and eukaryotic pathways of lipid synthesis in the '16:3' plant *Arabidopsis thaliana*. Biochem. J. **235:** 25–31.

Chen, J., Burke, J.J., Xin, Z., Xu, C., and Velten, J. (2006). Characterization of the *Arabidopsis* thermosensitive mutant *atts02* reveals an important role for galactolipids in thermotolerance. Plant Cell Environ. **29:** 1437–1448.

Cruz-Ramírez, A., Oropeza-Aburto, A., Razo-Hernández, F., Ramírez-Chávez, E., and Herrera-Estrella, L. (2006). Phospholipase DZ2 plays an important role in extraplastidic galactolipid biosynthesis and phosphate recycling in Arabidopsis roots. Proc. Natl. Acad. Sci. USA **103:** 6765–6770.

Dobin, A., Davis, C.A., Schlesinger, F., Drenkow, J., Zaleski, C., Jha, S., Batut, P., Chaisson, M., and Gingeras, T.R. (2013). STAR: ultrafast universal RNA-seq aligner. Bioinformatics **29:** 15–21.

Eastmond, P.J. (2006). *SUGAR-DEPENDENT1* encodes a patatin domain triacylglycerol lipase that initiates storage oil breakdown in germinating Arabidopsis seeds. Plant Cell **18:** 665–675.

Eastmond, P.J., Quettier, A.L., Kroon, J.T., Craddock, C., Adams, N., and Slabas, A.R. (2010). Phosphatidic acid phosphohydrolase 1 and 2 regulate phospholipid synthesis at the endoplasmic reticulum in Arabidopsis. Plant Cell **22:** 2796–2811.

El-Kouhen, K., Blangy, S., Ortiz, E., Gardies, A.M., Ferté, N., and Arondel, V. (2005). Identification and characterization of a triacylglycerol lipase in Arabidopsis homologous to mammalian acid lipases. FEBS Lett. **579:** 6067–6073.

Falcone, D.L., Ogas, J.P., and Somerville, C.R. (2004). Regulation of membrane fatty acid composition by temperature in mutants of *Arabidopsis* with alterations in membrane lipid composition. BMC Plant Biol. **4:** 17–32.

Fan, J., Yan, C., Zhang, X., and Xu, C. (2013). Dual role for phospholipid: diacylglycerol acyltransferase: enhancing fatty acid synthesis and diverting fatty acids from membrane lipids to triacylglycerol in Arabidopsis leaves. Plant Cell **25:** 3506–3518.

Fowler, D.B. (2008). Cold acclimation threshold induction temperatures in cereals. Crop Sci. **48:** 1147–1154.

Gasulla, F., Vom Dorp, K., Dombrink, I., Zähringer, U., Gisch, N., Dörmann, P., and Bartels, D. (2013). The role of lipid metabolism in the acquisition of desiccation tolerance in *Craterostigma plantagineum*: a comparative approach. Plant J. **75:** 726–741.

Grabherr, M.G., et al. (2011). Full-length transcriptome assembly from RNA-Seq data without a reference genome. Nat. Biotechnol. **29:** 644–652.

Haas, B.J., et al. (2013). *De novo* transcript sequence reconstruction from RNA-seq using the Trinity platform for reference generation and analysis. Nat. Protoc. **8:** 1494–1512.

Härtel, H., Dörmann, P., and Benning, C. (2000). DGD1-independent biosynthesis of extraplastidic galactolipids after phosphate deprivation in *Arabidopsis.* Proc. Natl. Acad. Sci. USA **97:** 10649–10654.

Harwood, J. (1991). Strategies for coping with low environmental temperatures. Trends Biochem. Sci. **16:** 126–127.

Harwood, J. (1994). Environmental factors which can alter lipid metabolism. Prog. Lipid Res. **33:** 193–202.

Heilmann, I., Mekhedov, S., King, B., Browse, J., and Shanklin, J. (2004). Identification of the Arabidopsis palmitoyl-monogalactosyldiacylglycerol delta7-desaturase gene FAD5, and effects of plastidial retargeting of Arabidopsis desaturases on the *fad5* mutant phenotype. Plant Physiol. **136:** 4237–4245.

Heinz, E., and Roughan, P.G. (1983). Similarities and differences in lipid metabolism of chloroplasts isolated from 18:3 and 16:3 plants. Plant Physiol. **72:** 273–279.

Heppard, E.P., Kinney, A.J., Stecca, K.L., and Miao, G.H. (1996). Developmental and growth temperature regulation of two different microsomal ω-6 desaturase genes in soybeans. Plant Physiol. **110:** 311–319.

Huang, D., Jaradat, M.R., Wu, W., Ambrose, S.J., Ross, A.R., Abrams, S.R., and Cutler, A.J. (2007). Structural analogs of ABA reveal novel features of ABA perception and signaling in Arabidopsis. Plant J. **50:** 414–428.

Huang, X., and Madan, A. (1999). CAP3: A DNA sequence assembly program. Genome Res. **9:** 868–877.

Hugly, S., Kunst, L., Browse, J., and Somerville, C. (1989). Enhanced thermal tolerance of photosynthesis and altered chloroplast ultrastructure in a mutant of Arabidopsis deficient in lipid desaturation. Plant Physiol. **90:** 1134–1142.

Hugly, S., and Somerville, C. (1992). A role for membrane lipid polyunsaturation in chloroplast biogenesis at low temperature. Plant Physiol. **99:** 197–202.

Iba, K. (2002). Acclimative response to temperature stress in higher plants: approaches of gene engineering for temperature tolerance. Annu. Rev. Plant Biol. **53:** 225–245.

International Wheat Genome Sequencing Consortium (IWGSC) (2014). A chromosome-based draft sequence of the hexaploid bread wheat (*Triticum aestivum*) genome. Science **345:** 1251788.

James, C.N., Horn, P.J., Case, C.R., Gidda, S.K., Zhang, D., Mullen, R.T., Dyer, J.M., Anderson, R.G., and Chapman, K.D. (2010). Disruption of the Arabidopsis CGI-58 homologue produces Chanarin-Dorfman-like lipid droplet accumulation in plants. Proc. Natl. Acad. Sci. USA **107:** 17833–17838.

Johnson, G., and Williams, J.P. (1989). Effect of growth temperature on the biosynthesis of chloroplastic galactosyldiacylglycerol molecular species in *Brassica napus* leaves. Plant Physiol. **91:** 924–929.

Katavic, V., Reed, D.W., Taylor, D.C., Giblin, E.M., Barton, D.L., Zou, J., Mackenzie, S.L., Covello, P.S., and Kunst, L. (1995). Alteration of seed fatty acid composition by an ethyl methanesulfonate-induced mutation in *Arabidopsis thaliana* affecting diacylglycerol acyltransferase activity. Plant Physiol. **108:** 399–409.

Kelly, A.A., Froehlich, J.E., and Dörmann, P. (2003). Disruption of the two digalactosyldiacylglycerol synthase genes DGD1 and DGD2 in *Arabidopsis* reveals the existence of an additional enzyme of galactolipid synthesis. Plant Cell **15:** 2694–2706.

Kong, Y. (2011). Btrim: a fast, lightweight adapter and quality trimming program for next-generation sequencing technologies. Genomics **98:** 152–153.

Kunst, L., Browse, J., and Somerville, C. (1988). Altered regulation of lipid biosynthesis in a mutant of *Arabidopsis* deficient in chloroplast glycerol-3-phosphate acyltransferase activity. Proc. Natl. Acad. Sci. USA **85:** 4143–4147.

Kunst, L., Browse, J., and Somerville, C. (1989). Enhanced thermal tolerance in a mutant of Arabidopsis deficient in palmitic Acid unsaturation. Plant Physiol. **91:** 401–408.

Langmead, B., and Salzberg, S.L. (2012). Fast gapped-read alignment with Bowtie 2. Nat. Methods **9:** 357–359.

Li, M., Welti, R., and Wang, X. (2006). Quantitative profiling of Arabidopsis polar glycerolipids in response to phosphorus starvation. Roles of phospholipases D zeta1 and D zeta2 in phosphatidylcholine hydrolysis and digalactosyldiacylglycerol accumulation in phosphorus-starved plants. Plant Physiol. **142:** 750–761.

Li-Beisson, Y., et al. (2013). Acyl-lipid metabolism. The Arabidopsis Book **11:** e0161, doi/10.1199/tab.0161.

Limin, A.E., and Fowler, D.B. (2006). Low-temperature tolerance and genetic potential in wheat (*Triticum aestivum* L.): response to photoperiod, vernalization, and plant development. Planta **224:** 360–366.

Matsuda, O., Sakamoto, H., Hashimoto, T., and Iba, K. (2005). A temperature-sensitive mechanism that regulates post-translational stability of a plastidial omega-3 fatty acid desaturase (FAD8) in Arabidopsis leaf tissues. J. Biol. Chem. **280:** 3597–3604.

McConn, M., and Browse, J. (1996). The critical requirement for linolenic acid is pollen development, not photosynthesis, in an Arabidopsis mutant. Plant Cell **8:** 403–416.

Miquel, M., and Browse, J. (1992). *Arabidopsis* mutants deficient in polyunsaturated fatty acid synthesis. Biochemical and genetic characterization of a plant oleoyl-phosphatidylcholine desaturase. J. Biol. Chem. **267:** 1502–1509.

Miquel, M., Cassagne, C., and Browse, J. (1998). A new class of Arabidopsis mutants with reduced hexadecatrienoic acid fatty acid levels. Plant Physiol. **117:** 923–930.

Miquel, M., James, D., Jr., Dooner, H., and Browse, J. (1993). Arabidopsis requires polyunsaturated lipids for low-temperature survival. Proc. Natl. Acad. Sci. USA **90:** 6208–6212.

Moellering, E.R., Muthan, B., and Benning, C. (2010). Freezing tolerance in plants requires lipid remodeling at the outer chloroplast membrane. Science **330:** 226–228.

Mongrand, S., Bessoule, J., Cabantous, F., and Cassagne, C. (1998). The $C_{16:3}/C_{18:3}$ fatty acid balance in photosynthetic tissues from 468 plant species. Phytochemistry **49:** 1049–1064.

Murakami, Y., Tsuyama, M., Kobayashi, Y., Kodama, H., and Iba, K. (2000). Trienoic fatty acids and plant tolerance of high temperature. Science **287:** 476–479.

Murata, N., and Los, D.A. (1997). Membrane fluidity and temperature perception. Plant Physiol. **115:** 875–879.

Murata, N., Ishizaki-Nishizawa, O., Higashi, S., Hayashi, H., Tasaka, Y., and Nishida, I. (1992). Genetically engineered alteration in the chilling sensitivity of plants. Nature **356:** 710–713.

Nakamura, Y., Awai, K., Masuda, T., Yoshioka, Y., Takamiya, K., and Ohta, H. (2005). A novel phosphatidylcholine-hydrolyzing phospholipase C induced by phosphate starvation in Arabidopsis. J. Biol. Chem. **280:** 7469–7476.

Ohlrogge, J., and Browse, J. (1995). Lipid biosynthesis. Plant Cell **7:** 957–970.

Ouyang, S., and Buell, C.R. (2004). The TIGR Plant Repeat Databases: a collective resource for the identification of repetitive sequences in plants. Nucleic Acids Res. **32:** D360–D363.

Pearcy, R.W. (1978). Effects of growth temperature on the fatty acid composition of the leaf lipids in *Atriplex lentiformis* (Torr.) Wats. Plant Physiol. **61:** 484–486.

Peters, C., Li, M., Narasimhan, R., Roth, M., Welti, R., and Wang, X. (2010). Nonspecific phospholipase C NPC4 promotes responses to abscisic acid and tolerance to hyperosmotic stress in Arabidopsis. Plant Cell **22:** 2642–2659.

Pinfield-Wells, H., Rylott, E.L., Gilday, A.D., Graham, S., Job, K., Larson, T.R., and Graham, I.A. (2005). Sucrose rescues seedling establishment but not germination of Arabidopsis mutants disrupted in peroxisomal fatty acid catabolism. Plant J. **43:** 861–872.

Reddy, V.S., Rao, D.K., and Rajasekharan, R. (2010). Functional characterization of lysophosphatidic acid phosphatase from *Arabidopsis thaliana.* Biochim. Biophys. Acta **1801:** 455–461.

Robinson, M.D., McCarthy, D.J., and Smyth, G.K. (2010). edgeR: a Bioconductor package for differential expression analysis of digital gene expression data. Bioinformatics **26:** 139–140.

Routaboul, J.M., Skidmore, C., Wallis, J.G., and Browse, J. (2012). Arabidopsis mutants reveal that short- and long-term thermotolerance have different requirements for trienoic fatty acids. J. Exp. Bot. **63:** 1435–1443.

Schnurr, J.A., Shockey, J.M., de Boer, G.J., and Browse, J.A. (2002). Fatty acid export from the chloroplast. Molecular characterization of a major plastidial acyl-coenzyme A synthetase from Arabidopsis. Plant Physiol. **129:** 1700–1709.

Shen, W., Li, J.Q., Dauk, M., Huang, Y., Periappuram, C., Wei, Y., and Zou, J. (2010). Metabolic and transcriptional responses of glycerolipid pathways to a perturbation of glycerol 3-phosphate metabolism in Arabidopsis. J. Biol. Chem. **285:** 22957–22965.

Somerville, C., and Browse, J. (1991). Plant lipids: metabolism, mutants, and membranes. Science **252:** 80–87.

Szymanski, J., Brotman, Y., Willmitzer, L., and Cuadros-Inostroza, Á. (2014). Linking gene expression and membrane lipid composition of Arabidopsis. Plant Cell **26:** 915–928.

Tang, G.Q., Novitzky, W.P., Carol Griffin, H., Huber, S.C., and Dewey, R.E. (2005). Oleate desaturase enzymes of soybean: evidence of regulation through differential stability and phosphorylation. Plant J. **44:** 433–446.

Trapnell, C., Roberts, A., Goff, L., Pertea, G., Kim, D., Kelley, D.R., Pimentel, H., Salzberg, S.L., Rinn, J.L., and Pachter, L. (2012).

Differential gene and transcript expression analysis of RNA-seq experiments with TopHat and Cufflinks. Nat. Protoc. **7:** 562–578.

Vergnolle, C., Vaultier, M.N., Taconnat, L., Renou, J.P., Kader, J.C., Zachowski, A., and Ruelland, E. (2005). The cold-induced early activation of phospholipase C and D pathways determines the response of two distinct clusters of genes in Arabidopsis cell suspensions. Plant Physiol. **139:** 1217–1233.

Wallis, J.G., and Browse, J. (2002). Mutants of *Arabidopsis* reveal many roles for membrane lipids. Prog. Lipid Res. **41:** 254–278.

Welti, R., Li, W., Li, M., Sang, Y., Biesiada, H., Zhou, H.E., Rajashekar, C.B., Williams, T.D., and Wang, X. (2002). Profiling membrane lipids in plant stress responses. Role of phospholipase D α in freezing-induced lipid changes in Arabidopsis. J. Biol. Chem. **277:** 31994–32002.

Winichayakul, S., Scott, R.W., Roldan, M., Hatier, J.H., Livingston, S., Cookson, R., Curran, A.C., and Roberts, N.J. (2013). *In vivo* packaging of triacylglycerols enhances Arabidopsis leaf biomass and energy density. Plant Physiol. **162:** 626–639.

Wolfe, J. (1978). Chilling injury in plants-the role of membrane lipid fluidity. Plant Cell Environ. **1:** 241–247.

Xu, C., Yu, B., Cornish, A.J., Froehlich, J.E., and Benning, C. (2006). Phosphatidylglycerol biosynthesis in chloroplasts of Arabidopsis mutants deficient in acyl-ACP glycerol-3- phosphate acyltransferase. Plant J. **47:** 296–309.

Zou, J., Wei, Y., Jako, C., Kumar, A., Selvaraj, G., and Taylor, D.C. (1999). The *Arabidopsis thaliana* TAG1 mutant has a mutation in a diacylglycerol acyltransferase gene. Plant J. **19:** 645–653.